THE EFFECT OF DISPERSED PHASE FEED RATE ON THE PRODUCTION OF PICKERING EMULSIONS

A THESIS SUBMITTED TO
THE GRADUATE SCHOOL OF NATURAL AND APPLIED SCIENCES
OF
MIDDLE EAST TECHNICAL UNIVERSITY

BY

DİLA DÖNMEZ

IN PARTIAL FULFILLMENT OF THE REQUIREMENTS
FOR
THE DEGREE OF MASTER OF SCIENCE
IN
CHEMICAL ENGINEERING

SEPTEMBER 2018

Approval of thesis:

THE EFFECT OF DISPERSED PHASE FEED RATE ON THE PRODUCTION OF PICKERING EMULSIONS

submitted by **DİLA DÖNMEZ** in partial fulfillment of the requirements for the degree of **Master of Science in Chemical Engineering Department, Middle East Technical University** by,

Prof. Dr. Halil Kalıpçılar _____
Dean, Graduate School of **Natural and Applied Sciences**

Prof. Dr. Pınar Çalık _____
Head of Department, **Chemical Engineering**

Asst. Prof. Dr. İnci Ayrancı _____
Supervisor, **Chemical Engineering Dept., METU**

Examining Committee Members:

Prof. Dr. Yusuf Uludağ _____
Chemical Engineering Dept., METU

Asst. Prof. Dr. İnci Ayrancı _____
Chemical Engineering Dept., METU

Prof. Dr. Nihal Aydoğan _____
Chemical Engineering Dept., Hacettepe University

Assoc. Prof. Dr. Görkem Külah _____
Chemical Engineering Dept., METU

Asst. Prof. Dr. Emre Büküşoğlu _____
Chemical Engineering Dept., METU

Date: 05/09/2018

I hereby declare that all information in this document has been obtained and presented in accordance with academic rules and ethical conduct. I also declare that, as required by these rules and conduct, I have fully cited and referenced all material and results that are not original to this work.

Name, Last name:

Signature :

ABSTRACT

THE EFFECT OF DISPERSED PHASE FEED RATE ON THE PRODUCTION OF PICKERING EMULSIONS

Dönmez, Dila
M. Sc., Department of Chemical Engineering
Supervisor: Asst. Prof. Dr. İnci Ayrancı

September 2018, 81 Pages

Emulsions are fundamental in many applications such as food, petroleum, detergent, pharmaceutical and cosmetic industries. Pickering emulsions are defined as emulsions of any type, either oil-in water, water-in-oil or even multiple, stabilized by solid particles instead of surfactants. Solid particles may prevent the droplets from coalescing by getting adsorbed at the interface, and thus stabilizing the emulsion. Pickering emulsions have more advantages over emulsions stabilized by surfactants in terms of stability, biocompatibility, environmental risks and cost.

There are numerous studies about the effect of oil, water and particle properties, but almost no studies about the effect of processing parameters on the formation of Pickering emulsions in a stirred tank. The literature shows that the feed rate of a second phase into the first one has a significant impact on the mixing process, and therefore the product properties. This also applies to formation of Pickering emulsions: the feed rate of the dispersed phase into the continuous phase may be a critical processing parameter that impacts the final droplet size. In this study, the aim was to investigate the effect of feed rate of the oil phase on the final average droplet size when the following hydrodynamic conditions were constant for all configurations: tip speed, power per mass, impeller Reynolds number. Pickering emulsions were produced by using silicone oil as dispersed phase, distilled water as continuous phase, calcite as an emulsifier in a stirred tank where the feed rate of the

dispersed phase was varied. The experiments were performed with three different impellers: Rushton turbine (RT), up-pumping pitched blade turbine (PBTU), and down-pumping pitched blade turbine (PBTD). All the impellers were tested at two different sizes, T/3 and T/2 where T is the tank diameter. The droplet diameters were measured in Mastersizer® 3000 (Malvern) which is a particle size analyzer.

In summary, it was found that the decrease in feed rate causes reduction in the average droplets size due to smaller newly generated droplets and effective particle adsorption. This is only valid if the droplets have not reached the minimum equilibrium size at different hydrodynamic conditions. At lower impeller speeds and feed rates, the effect of feed rate is more pronounced, thereby under these conditions, maximum reduction in the average droplet size is found as 24% with RT-T/3. Besides of the feed rate effect, it was also found that impeller type, impeller size, feeding point and hydrodynamic conditions have an impact on the average droplet size.

Keywords: Pickering emulsions, feed rate, solid particles, stirred tanks, mixing.

ÖZ

DAĞILAN FAZ BESLEME HIZININ PİCKERİNG EMÜLSİYONU OLUŞUMUNA ETKİSİ

Dönmez, Dila
Yüksek Lisans, Kimya Mühendisliği Bölümü
Tez Yöneticisi: Dr. Öğr. Üyesi İnci Ayrancı

Eylül 2018, 81 sayfa

Emülsiyonlar, gıda, petrol, deterjan, ilaç ve kozmetik endüstrileri gibi birçok uygulamada temeldir. Pickering emülsiyonları sürfaktanlar yerine katı partiküller ile stabilize edilmiş: yağ-içinde-su, su-içinde-yağ hatta çoklu emülsiyonlar olarak tanımlanabilir. Katı partiküller, ara yüzeyde adsorbe olarak, damlacıkların birleşmesini önleyebilirler ve böylece emülsiyonu stabilize ederler. Pickering emülsiyonları, yüzey aktif maddeler tarafından stabilize edilen emülsiyonlara göre stabilite, biyouyumluluk, çevresel riskler ve maliyet açısından daha avantajlıdır.

Yağ, su ve partikül özelliklerinin etkisi hakkında çok sayıda çalışma vardır, ancak proses parametrelerinin, Pickering emülsiyonlarının bir karıştırmalı tankta oluşumuna etkisi hakkında neredeyse hiç bir çalışma yoktur. Özellikle, ikinci fazın birinci faza olan besleme hızının, karıştırma işlemi ve dolayısıyla ürün özellikleri üzerinde önemli bir etkiye sahip olduğu literatürde gösterilmiştir. Bu durum aynı zamanda, Pickering emülsiyonlarının oluşumu için de geçerlidir bu sebeple dağılan fazın sürekli faza besleme hızı, nihai damlacık boyutunu etkileyen kritik bir işlem parametresi olabilir. Bu çalışmada amaç, bütün konfigürasyonlar için aşağıdaki hidrodinamik koşullar sabit olduğunda: bıçak Reynolds sayısı, uç hızı, kütle başına güç, yağ fazının besleme hızının son damlacık boyutuna etkisini araştırmaktır. Dağılan fazın besleme hızının değiştiği karıştırmalı bir tankta Pickering

emülsiyonları üretilmiştir; dağılan faz olarak silikon yağı, sürekli faz olarak damıtılmış su, emülgatör olarak kalsit kullanılmıştır. Deneyler üç farklı bıçak türü ile gerçekleştirilmiştir: Rushton türbin (RT), yukarı pompalayan eğimli bıçak türbin (PBTU) ve aşağı pompalayan eğimli bıçak türbin (PBTD). Tüm bıçaklar, T'nin tank çapı olduğu iki farklı boyutta, T/3 ve T/2 ' de test edildi. Damlacık çapları partikül boyutu analizörü olan Mastersizer® 3000 (Malvern)'de ölçüldü.

Özetle, besleme hızındaki azalmanın, yeni oluşturulan küçük damlacıklar ve etkili parçacık adsorpsiyonu nedeniyle ortalama damlacıkların boyutunda azalmaya neden olduğu bulunmuştur. Bu durum, sadece damlacıkların farklı hidrodinamik koşullardaki minimum denge büyüklüğüne ulaşmamış olması durumunda geçerlidir. Daha düşük bıçak ve besleme hızlarında, besleme hızının etkisi daha belirgindir, dolayısıyla bu koşullar altında ortalama damlacık boyutunda maksimum azalma RT-T/3 ile % 24 olarak bulunmuştur. Besleme hızının etkisinin yanı sıra, bıçak tipi, bıçak boyutu, besleme noktası ve hidrodinamik koşulların, ortalama damlacık boyutu üzerinde bir etkisi olduğu bulunmuştur.

Anahtar kelimeler: Pickering emülsiyonları, besleme hızı, katı partiküller, karıştırmalı tank, karıştırma

Dedicated to my husband, Ata Donmez and my family

ACKNOWLEDGEMENTS

First, I would like to express my special thanks to my supervisor Asst. Prof. Dr. İnci Ayranci for her endless kind support, guidance, comments and suggestions throughout my thesis study. Her contributions are sincerely appreciated and gratefully acknowledged.

I am greatly thankful to members of Multiphase Mixing Research Laboratory, METU especially Usman Kayode Abdulrasaq and Özge Demirdoğan for their friendship and support. Also, I would like to thank to Asst. Prof. Dr. Emre Büküşoğlu and his lab members for helping me about getting microscope images of particles and droplets.

I want to thank my whole family especially, my mother, Hülya Karakaya, my father, Muharrem Karakaya, and my sister, Rüya Karakaya Erdoğan for their endless support in every aspect throughout my life. Also, my dear friends, Melike Bayana, Zeliha Yolun, Omar Wehbe and Esra Kanmaz encouraged me throughout the study.

Finally, I would like to express my special gratitude my lovely spouse, Ata Dönmez for his kind cooperation about setting digital controller for the peristaltic pump and his endless encouragement which helped me in the completion of this study.

This study is supported by METU BAP, I thank them for the financial support. BAP Grant no:03-04-2017-003.

TABLE OF CONTENTS

LIST OF TABLES

TABLES

LIST OF FIGURES

FIGURES

LIST OF SYMBOLS

Roman Characters

T: tank diameter (m)

C: off-bottom clearance of the impeller (m)

D: diameter of impeller (m)

H: liquid height (m)

d: droplet diameter (μm)

N: rotational speed of the impeller (rev/s)

Z: distance from the bottom of the tank (m)

r: distance from the shaft of the tank (m)

P: power consumption (J/s)

Np: power number (-)

V_{tip}: tip speed (m/s)

n_i: the number of droplets

d_i: the nominal diameter of droplets (μm)

d_{feed}: diameter of the feed tube (mm)

P_L: Laplace pressure (Pa)

d_{max}: the maximum stable droplet size (μm)

$\varepsilon_{t,max}$: maximum local energy dissipation rate

d_{32}: Sauter mean diameter (μm)

d_{43}: volume mean diameter (μm)

V_{swept}: impeller swept volume (m^3)

γ_{ow}: oil/water interfacial tension (N/m)

Φ_s: volume fraction of calcite particles

η_r: relative viscosity

μ_s: viscosity of suspension (kg/ms)

μ_c: viscosity of continuous fluid (kg/ms)

W: baffle width (m)

W_{set}: the desired weight of the silicone oil fed into the tank (kg)

$W_{instaneous}$: the weight measured at an instant (kg)

W_i: initial weight of the reservoir (kg)

W_f: final weight of the reservoir (kg)

V_{motor}: applied voltage to electric motor of the pump

$\dot{m}$: flow rate of the silicone oil

G_p: process transfer function

G_c: controller transfer function

H: sensor/ transmitter transfer function

Greek Characters

μ: dynamic viscosity of the liquid (kg/ms)

ρ: density of the liquid (kg/m^3)

σ: surface tension (N/m)

Θ: contact angle

LIST OF ABBREVIATIONS

PBT: pitched blade turbine

PBTD: down-pumping pitched blade turbine

PBTU: up-pumping pitched blade turbine

RT: Rushton turbine

wt. %: weight percent

v/v %: volume/volume percent

o/w: oil in water

w/o: water in oil

Re: Reynolds number

We: Weber number

PPM: power per mass

PWM: pulse width modulation

DLVO: Derjaguin, Landau, Verwey and Overbeek

CHAPTER 1

INTRODUCTION AND LITERATURE REVIEW

1.1 Mixing

Mixing is a physical operation that reduces non-uniformities to achieve desired process results. The non-uniformities are concentration, phase or temperature distribution etc. Critical objectives such as mass transfer rate, reaction yield or properties of products can be affected from these non-uniformities (Paul et al., 2004). The equipment used for mixing has substantial effect on agitation efficiency which affect product quality and yield, power consumption and cost of manufacturing. If proper mixing is not conducted, product failure would occur. The result of failure may also cause stock-out and cancellation of the product that return as tremendous cost. These issues show that proper design of mixing equipment is critical for processes. There are various core mixing design topics : homogenous blending in tanks or in-line mixers, dispersion of gases in liquids, solid-liquid suspension, miscible and immiscible liquid-liquid dispersion, heat transfer, homogenous and heterogenous reactions (Paul et al.,2004). In this study, a type of immiscible liquid-liquid dispersion - production of Pickering emulsions -is targeted. In the following sections, first details of immiscible liquid-liquid mixing without solid particles, then the production of Pickering emulsions are explained.

1.2 Immiscible Liquid-Liquid Mixing

Liquid-liquid-mixing is substantial for generation of new interfacial area to enhance mass and heat transfer between the phases (O'Rourke & MacLoughlin, 2005). Liquid-liquid mixing can be examined in two groups: miscible and immiscible. ''Blending'' term is used for miscible liquid-liquid system and ''Mixing'' term is used for immiscible liquid-liquid dispersions or production of emulsions (Jakobsen, 2008). Emulsions can be defined as a mixture of two or more insoluble liquids, which

are usually oil and water. Oil or water droplets -depending on the structure of emulsion- are generated by agitation. Emulsion structure can be oil suspended in water (o/w) or water suspended in oil (w/o). These emulsions are also called as oil-in-water or water-in-oil emulsions. Droplets can be stabilized either by surfactants or solid particles; therefore emulsions are classified based on its stabilizer (emulsifier) type: surfactant-based emulsions or solid-stabilized emulsions which are also called as Pickering emulsions (Leng & Calabrese, 2004).

An immiscible liquid-liquid system refers to presence of two or more insoluble phases as partitioned phases. These phases are called as dispersed phase and continuous phase. The dispersed phase has usually smaller volume compared to continuous phase (Leng & Calabrese, 2004).

To create immiscible liquid-liquid dispersions, stirred tanks or other equipment can be utilized. Agitation controls the droplet breakage – also known as dispersion – and merging of droplets – also known as coalescence – and droplet suspension within the system. The mixing intensity and flow direction produced by an impeller affect the size and distribution of the droplets throughout the tank besides the dispersion kinetics. Lower turbulences or laminar conditions in the tank promote coalescence by increasing contact time of droplets. However, laminar conditions may also cause dispersion of droplets if the droplets exceed the point of critical elongation, following which droplet break-up occurs (Leng & Calabrese, 2004). This shows that the hydrodynamic regime and details of hydrodynamics are very important in creating immiscible liquid-liquid dispersions. The hydrodynamics are mainly determined by the equipment used.

Various types of equipment such as stirred tanks, static mixers, rotor/stator systems and colloid mills can be the choice for immiscible liquid-liquid dispersions; however, stirred tanks are the most attainable and comprehensive equipment utilized in many processes due to their high shear characteristics. In stirred tanks, high pumping capacity of impellers improves natural diffusivity of the liquids; therefore, it is important to choose the best impeller for the operation under consideration. Incorrect selection of the tank system may lead to poor product quality and higher power

consumption that lead to an increase in manufacturing cost as explained before (Afshar Ghotli et al., 2013).

1.2.1 Industrial Applications of Immiscible Liquid-Liquid Mixing

Immiscible liquid-liquid systems are widely used in many industries such as chemical, petroleum and pharmaceutical. The applications can be divided into two main groups: applications with chemical reactions or only dispersion. For the first group, the rate of reactions depends on mass transfer and influenced from interfacial area. The examples are hydrogenation, sulfonation, alkylation and nitration (Leng & Calabrese, 2004). In this thesis, applications of immiscible liquid-liquid systems without reactions which belongs to the second group are considered. These systems are also known as emulsions. Emulsions are used in different industries. Emulsion products include foods such as dairy milk and mayonnaise, personal care creams and lotions, insulating materials, polishes, drugs, paints, cosmetics etc. A range of food-grade particles which are wax crystals, calcite, ethyl cellulose, protein-polysaccharide complexes, fat crystals etc. was investigated to be utilized in emulsion stabilization. Many food products such as mayonnaise, margarine, whipped cream, butter, ice cream are, in fact, entirely or partially stabilized by the sub-micron sized particles (Pawlik et al., 2016).

In pharmaceutical application, biocompatible solid particles such as chitosan (CS), cyclodextrin (CD), and food-grade materials are used to stabilize Pickering emulsions. Therefore, emulsion products with these particles are more biodegradable and suitable for use in vivo (Frelichowska et al., 2009). Another application in pharmaceutical industry is proper drug delivery and release of its active materials to specific sites without any side effects (Marto et al., 2015) .

In cosmetic industry, emulsions have been most commonly used by far. Cosmetic emulsions are applied through surface of skin which is epidermis. They are limited with surface of the skin unlike pharmaceutical active ingredients which diffuse entire body or act locally after deep penetration.

In agriculture industry, active substances for treating plants and soils are usually produced as emulsions, i.e. pesticides and herbicides. (Chappat, 1994).

One other type of application of emulsions is to provide permanent and transient antifoams to processes such as cosmetics, foods, pulp and paper, pharmaceuticals, water treatment and minerals beneficiation (Dickinson, 1987; Everett, 1988; Mysels, 1959).

1.2.2 The Equipment for Immiscible Liquid-Liquid Systems

Mixing is usually carried out on stirred tanks as it was in this study. Stirred tanks may or may not include baffles. Baffles can be defined as metal vertical strips attached the wall of the tank. They are utilized for decreasing vortex and swirling of the liquid. One or multiple impellers can be installed on a centered stirrer shaft with baffles or off-centered stirrer shaft without baffles (Doran, 2013). The stirrer motor is connected with the shaft. The function of rotating impeller is to pump the liquid through the tank and create a flow pattern. The flow pattern of the impeller can be commonly explained as follows: when the liquid is pumped away from the impeller, it is circulated through the tank, and regularly returns to the impeller zone. Mixing can be accomplished using batch, semi-batch and continuous modes. For the continuous and semi-batch modes, feed tubes are often used (Doran, 2013).

1.2.3 Mixers

Although the scope of present study is about Pickering emulsion production in a baffled stirrer tank with different type of impellers, other mixers are also stated in this section. Various types of mixers are used for immiscible liquid-liquid systems in industry: stirred tanks, static mixers, rotor/stator systems, colloid mills, membranes and ultrasonic systems (Tsabet, 2014). The mixers are commonly selected based on drop size classification as shown in Table 1-1 or power consumption.

Table 1-1: Droplet size classification and droplet stability for various type of mixers*.

Droplet Size	Suitable Mixer	Stability
30 and 300 microns	Stirred tanks or static mixers	Less stable
A few microns	Rotor/stator systems and colloidal mills	Marginally stable
A hundred nanometers	Membranes or ultrasonic systems	Least stable

*Table 1-1 is reproduced from (Leng & Calabrese, 2004)

As explained in Section 1.2, stirred tanks have the lowest power consumption compared to other mixer that are used for immiscible liquid-liquid systems. The drawback of stirred tanks is that it produces larger average droplet sizes and they make usually less stable emulsions than others. The mixer decision should be based on obtaining the desired end-product quality with low power consumption.

1.2.3.1 Stirred Tank Geometry

Figure 1-1 shows a general stirred tank geometry, highlighting the parameters that affect mixing efficiency. For efficient mixing, a single impeller with a diameter (D) between 1/4 and 1/2 of tank diameter (T) can be used. The height of liquid in the tank (H) should not exceed 1.25T because mixing intensity reduces rapidly as fluid moves away from the impeller region and the liquid in the upper parts of the tank may remain unmixed. Another concern of tank geometry affecting mixing efficiency is the off-bottom clearance (C) which is defined as the distance between the impeller and bottom of the tank. In practical mixing operations, clearance is in between 1/6 and 1/2 of the tank diameter (Doran, 2013).

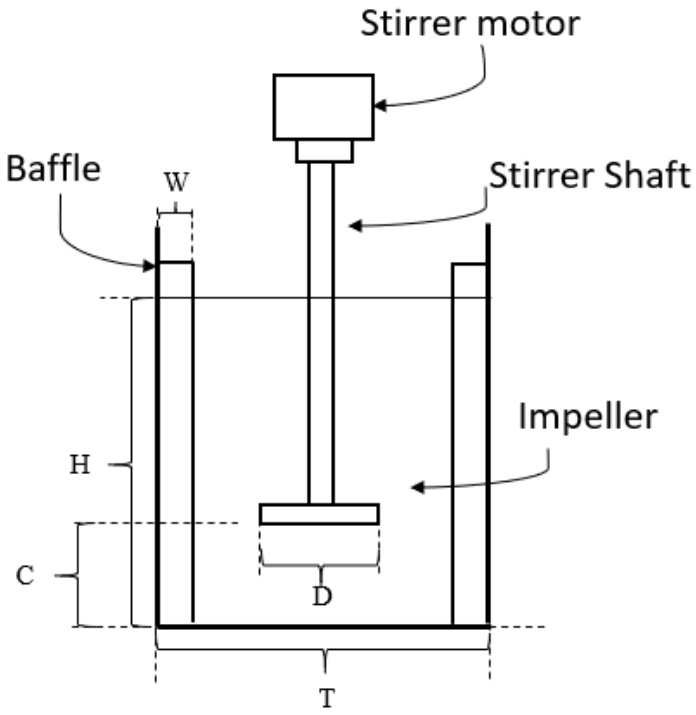

Figure 1-1: The representation of standard stirred tank geometry.

Baffles are essential part of the stirred tank when the shaft is centered. They increase mixing efficiency by preventing liquid swirling motion (solid body rotation) and vortex formation. Baffles assist generation of axial flow and turbulence in the tank by breaking up the circular flow created with impeller rotation. A standard baffle configuration includes four equally spaced vertical plates. The optimum baffle width depends on the impeller design and viscosity of the fluid, but it is generally 1/10 or 1/12 of the tank diameter (Doran, 2013) .

1.2.4 Impeller Types and Flow Patterns

In industry, hundreds of impeller types are used based on process requirements. In immiscible liquid-liquid mixing (low to medium viscosity), the common type is turbine impellers. Turbine impellers are usually characterized by flow patterns as follows (Hemrajani & Gary B., 2004);

- Axial flow impellers: Hydrofoil Impeller, Lightnin A-310, Chemineer HE-3, Marine Propeller
- Radial flow impellers: Rushton Turbine (RT), Flat Blade Turbine (FBT), Smith Impeller, Backswept Turbine
- Mixed flow impellers: Pitched Blade Turbine (PBT)

Among these impellers, the mixed flow impellers are used for solid incorporation and draw down of oil in the aspect of emulsification. Also, radial flow impellers are the most effective impeller in terms of liquid-liquid dispersion due to higher shear and turbulence level (Hemrajani & Gary B., 2004). The axial flow impellers are good for solids suspension, but they are not effective for dispersion of droplets. This makes the radial and mixed flow impellers good candidates for Pickering emulsions production. The two most common types of these two classes of impellers are explained in more detail below.

Pitched blade turbine (PBT) is a type of mixed flow impeller. A PBT includes a hub with four blades. The most common blade angle is 45º, but 30º and 60º angles are also used. In most applications, down-pumping pitched blade turbine (PBTD) is preferred due to lower energy consumption compared to RT. In addition, it has lower mixing time which is explained in Section 1.3.2 compared to up-pumping pitched blade turbine (PBTU) (Pacek et al., 1999).

Flow patterns of PBTD and PBTU are shown in Figure 1-2a and 1-2b. The discharge from both PBTD and PBTU has two components: axial and radial flow velocity. PBTD creates one circulation loop. The liquid is first pumped towards the bottom of the tank at the same angle as the blades. It is then directed upwards with the help of the baffles. PBTU has also one circulation loop, however; this time the fluid is first pumped upwards towards the surface as can be seen in Figure 1-2b. For applications such as gas dispersion or draw down of floating solids, up-pumping pitched blade turbine (PBTU) may be more effective (Hemrajani & Gary B., 2004). RT is a type of radial flow impeller. The Rushton turbine consists six vertical blades on the disk. RT produces two strong circulating loops, one below and one above the impeller as seen in Figure 1-2c.

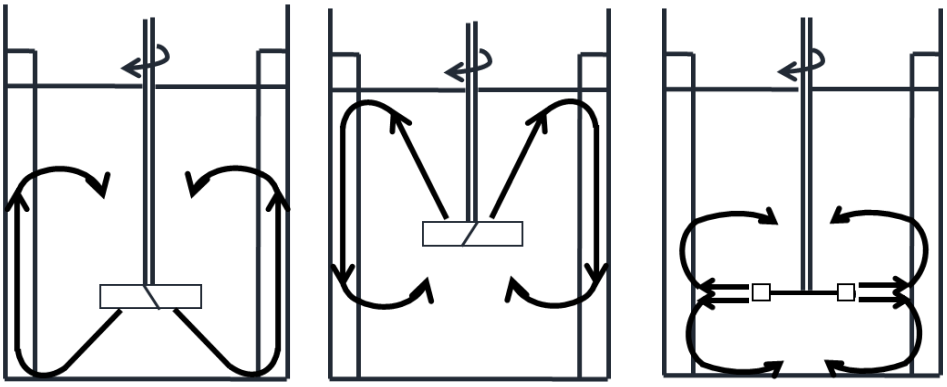

a. b. c.

Figure 1-2: Flow patterns of the various impellers: a. PBTD, b. PBTU and c. RT.

1.2.5 Feed Tube and Feed Tube Positions

Mixing in stirred tanks can be carried out in continuous, batch, or fed-batch mode. In fed-batch mode and continuous modes, feed tubes, or sometimes called as dip tubes, are used. In reaction environment, usage of feed tube reduces by-product formation. However, feed tubes may bring some problems in stirred tanks such as mechanical, metallurgical and operational (Bhattacharya & Kresta, 2004).

For immiscible liquid-liquid dispersion, the usage of feed tubes may be effective compared to surface feed as one phase needs to be dispersed in the other one. Energy dissipation rate, which is defined as the parameter that is used for determining the amount of energy lost by viscous forces, is a significant parameter to determine location of feed tubes. Podgórska (2009) stated that droplet breakage takes place in the impeller zone since the local dissipation rate is the highest in impeller vicinity and higher local dissipation rates (the point of most intense mixing) make the droplets smaller. Based on this information feeding of the oil can be done in the impeller zone.

The maximum dissipation points in the impeller region vary for each type of impeller. Feeding should be done at the points where the local level of turbulence is close to the maximum, or in other words at the maximum energy dissipation points. For single liquid phase systems, the maximum energy dissipation points with various impellers

were studied widely. The point is determined based on the radial and axial positions for each type of impeller. For the RT, the maximum energy dissipation point is 2r/D=1.08 in the radial position where r is the distance between the center of the tank and the tank wall; z/H=0.36 in the axial position where z is the distance from the tank bottom (Zhou & Kresta, 1996). Similarly, for the PBTD the maximum energy dissipation point is 2r/D=0.9 in the radial and z/H=0.28 in the axial position (Zhou & Kresta, 1996), and for the PBTU 2r/D=0.55 in the radial and z/H=0.42 (Amira, 2013).

1.3 Significant Parameters for Immiscible Liquid-Liquid Mixing

1.3.1 Mixing time

Mixing time is an important parameter to define degree of uniformity. Mixing time can be determined with the several methods such as the decolorization reaction of iodine and sodium thio-sulfate in water, electrical conductivity probes, acid-base neutralization reaction etc. (Ghotli et al., 2013). These methods are based on visual observation by adding small amount of tracer into the fluid. Some tracers such as hot water, sodium chloride solution or fluorescent dye are commonly utilized for determining the mixing time (Ghotli et al., 2013).

In immiscible liquid-liquid dispersion, the average droplet size is significantly affected by the mixing time. There are certain parameters that affect the mixing time: impeller speed, diameter of impellers and tanks, impeller types, number of baffles and fluid characteristics (Jakobsen, 2008). For example, Zhao et al. (2011) studied the effect of impeller type on mixing time. It is stated that PBTU has longer the mixing time compared to RT and PBTD in kerosene-water system. When the PBTU pumps the fluid upward, kerosene tends to coalesce and stay on the surface since it is lighter than water. This causes poor dispersion of the oil which increases the mixing time and makes the droplets bigger.

1.3.2 Circulation Time

The circulation time defines the time required for bulk fluid to leave and return to the impeller zone. On the other hand, mixing time determines the time when the system reaches uniformity in macro-scale. In general, the circulation time is significantly

shorter than mixing time in a tank (Jakobsen, 2008). For example, Tsabet & Fradette (2015) indicated that mixing time for an immiscible liquid-liquid system in a stirred tank is approximately five times of the circulation time. Since the circulation time is related to the mixing time, it has also significant effect on the average droplet size. Pacek et al. (1999) stated that thanks to shorter circulation time which means that the droplets move to the impeller zone more often, the low power number impeller which is PBTD produces smaller average droplet size for the same power per mass.

1.3.3 Dimensionless Numbers for Fluid Flow in Immiscible Liquid-liquid Systems

Several dimensionless numbers are used to classify flow in stirred tanks. The most common ones for immiscible liquid-liquid dispersion applications in stirred tanks are the Reynolds number and Weber number.

Reynolds number provides information about the ratio of inertial forces, those that accelerate motion of fluid against frictional forces, to viscous forces, those that slow the fluid motion down. In stirred tanks, Reynolds number is calculated with:

$$\mathrm{Re} = \frac{\mathrm{N}\mathrm{D}^2\rho}{\mu} \tag{1.1}$$

where ρ is the density of the fluid, μ is the molecular or dynamic viscosity of the fluid, N is the impeller speed and D is the impeller diameter. Flow regimes can be determined based on the impeller Reynolds number. If the impeller Reynolds number is smaller than 10, than the flow is laminar and if it is greater than $2x10^4$, the flow is turbulent. In turbulent regime, the behavior of two fluids at the same impeller Reynolds number is expected to be the similar in geometrically similar systems (Marden & Bakker, 2004).

During the agitation of two immiscible fluids, continuous break-up and coalescence of droplets occurs. The droplets are assumed to be broken by viscous shear forces or turbulent pressure fluctuations. Because of the interfacial tension, elastic stress is formed that means the droplets tend to stay in their original shape (Zhou, 1997). The

ratio of turbulent pressure fluctuations and the elastic stress is defined as the Weber number. It is shown in the following formula for stirred tanks;

$$We = \frac{\rho N^2 D^3}{\sigma} \tag{1.2}$$

where ρ is the density of the fluid, N is the impeller speed and D is the impeller diameter, σ is the surface tension (Zhou, 1997).

In immiscible liquid-liquid dispersions, Weber number is one of the most significant marker of droplet breakage condition. At high impeller Reynolds numbers, Weber number is correlated with the average droplet size and details of correlations are given in Section 1.3.5.

1.3.4 Power Consumption

The power drawn for the agitation shows close relationship between tank diameter (T) and impeller speed (N) for low viscosity fluids. Power number (N_p) has also significant effect on power consumption. The power number relates applied forces to inertial forces. Power number (N_p) varies based on the impeller type. For example, for RT and PBT, it can be taken as 5.2 and 1.3, respectively (Weetman, 2004).

The power consumption can be calculated from the following formula;

$$P = N_p \rho N^3 D^5 \tag{1.3}$$

Accordingly, power consumption mainly depends on stirred tank geometry, baffle design, characteristics of impeller, speed of impeller and type of fluid (Jakobsen, 2008). As an example, the stirred tank with radial flow impeller generates stronger circulation throughout the tank than the axial flow impellers. This causes increase in power consumption (Oldshue et al., 1986).

1.3.5 Droplet Size Distribution

Droplet size distribution of emulsions is defined usually a typical mean diameter based on statistical analysis. Here mean diameters are defined as following (Leng & Calabrese, 2004)

- **Arithmetic mean diameter (d_{10}, d_{50}, d_{90}):** d_{10} is defined as 10% by volume of all droplets smaller than d_{10}, d_{50} as 50% by volume of all droplets smaller than d_{50}, d_{90} as 90% by volume of all droplets smaller than d_{90}. These droplet diameters are determined from the cumulative volume frequency of the size distribution.

$$d_n = \frac{\sum_i n_i d_i}{\sum_i n_i} \tag{1.4}$$

- **The Sauter (Surface) mean diameter (d_{32}):** For the measurement of average droplet size, droplets can be represented in terms of d_{32}. d_{32} is a marker of surface area and smaller droplets which have high surface area affects significantly the Sauter mean diameter (Larsson & Friberg, 1990).

$$d_{32} = \frac{\sum_i n_i d_i^3}{\sum_i n_i d_i^2} \tag{1.5}$$

- **Volume mean diameter (d_{43}):** d_{43} is also used for measurement of average droplet size. Unlike d_{32} , d_{43} can measure small amounts of flocculation or coalescence in a polydisperse emulsion with volume-based considerations (Larsson & Friberg, 1990).

$$d_{43} = \frac{\sum_i n_i d_i^4}{\sum_i n_i d_i^3} \tag{1.6}$$

where n_i the number of droplets, d_i the nominal diameter of droplets in size class i.

Deforming stresses which have significant roles on breakage of droplets are defined in here. Normal and tangential stresses lead to deformation in the interface of the continuous and dispersed phases. However, the diameter of a spherical droplet (d) may tolerate a strain as intense as the pressure difference across the surface of the droplet, known as Laplace pressure (P_L) (Ghotli et al., 2013; Lemenand et al., 2003).

$$P_L = \frac{4\sigma}{d} \tag{1.7}$$

In turbulent regime, a droplet diameter may reach an equilibrium point where deforming stresses do not decrease droplet size and overcoming Laplace pressure is difficult. The maximum stability of droplet diameter in the impeller vicinity is called as maximum diameter, d_{max}. Therefore, under equilibrium conditions, droplet size distribution is not a function of time. If a droplet diameter is significantly larger than $d_{max,}$ it will eventually break-up in a short time. However, if it is larger than minimum diameter (d_{min}), droplets will coalesce.

Several studies have been conducted to develop correlations for predicting average droplet size for liquid-liquid dispersions. In most of the studies, the maximum stable droplet size (d_{max}) were related to maximum local energy dissipation rate ($\varepsilon_{t,max}$) (Hinze, 1955).

$$d_{max} = const.x\ (\varepsilon_{t,max})^{-0.4} \tag{1.8}$$

Hinze (1955), Chen et al. (1967), and Calabrese et al. (1986) assumed that Sauter mean diameter is linear function of the maximum stable droplet diameter.

$$d_{32} = const.x\ d_{max} \tag{1.9}$$

Those studies correlated Sauter mean diameter to the Weber number using the following general formula (Tsabet, 2014) ;

$$d_{32} \sim We^{-0.6} \ldots \tag{1.10}$$

However, this general formula is usually limited to specific conditions. Davies (1985) used the concept of McManamey (1979) and stated that maximum local energy dissipation rate ($\varepsilon_{t,max}$) should be based on the assumption that the rate of energy input or power (P) was dissipated in impeller swept volume (V_{swept}), which is defined as the region between the neighboring blades of the impeller (Yoshida et al., 2015). Power (P) dissipated in impeller swept volume (V_{swept}) is also called as power per mass (PPM) and the following formula represents the relation;

$$\varepsilon_{t,max} = \frac{P}{\rho V_{swept}} \quad (1.11)$$

This is only valid for impeller zone. However, the average droplet size that is obtained experimentally represents the entire mass in the tank including bulk of the tank as well as the impeller zone. This indicates that a gap between the model and the real situation (Zhou et al.,1998). For extremely viscous droplets, Calabrese et al. (1986) stated that no model based on power per unit mass of liquid ($P/\rho V_{swept}$) provide a reasonable correlation. Zhou et al. (1998) and EL-Hamouz et al. (2009) also argued that Sauter mean diameter (d_{32}) is not related to power per mass of liquid ($P/\rho V_{swept}$) when the operating parameters are changed. They found that mean flow (ND) is more reasonable than $P/\rho V_{swept}$ to correlate average droplet size.

$$d_{32} \sim ND \quad (1.12)$$

This shows that a range of parameters are candidates for relating the average droplet size to a hydrodynamic parameter for better design. These literature findings are for liquid-liquid dispersion systems where a surfactant, whether chemical or particle, does not exist. Pickering emulsions are much more complicated than these systems as particles should be suspended, oil should be dispersed, and particles should adsorb at the oil/water interphase simultaneously; therefore, a detailed analysis on the relevant hydrodynamic parameters is needed.

1.4 The Mechanisms of Droplet Break-up and Coalescence

The mechanism of droplet breakup and coalescence are two fundamental phenomena that determine the performance of turbulent liquid-liquid dispersions. Droplet deformation is caused by mechanical forces induced by the surrounding fluid and is prevented by surface and internal viscous forces. Droplet breakage occurs when fluid forces exceed the resistance forces (Leng & Calabrese, 2004).

Droplet break-up occurs in stages. Firstly, a type of immiscible liquid is dispersed into another liquid in the tank by an impeller. Fluid bulk continues deforming and breaks into chunks of fluid which are broken further into finer parts after the dispersion of liquids. Hinze (1955) stated a mechanism for disintegration of liquids and that is penetration of ligaments of one fluid to another. The ligaments break-up

into droplets which may split up into smaller parts. Since the thickness of ligaments are not equal during the disintegration process, droplets would be formed in different sizes. Hinze (1955) classified break-up processes into three types. This classification is based on visual observation of droplet breakup. Impact droplet collisions (walls, impeller blades, and baffles) lead to lenticular deformation, uniform shear cause to elongated deformation, and turbulent conditions cause to bulgy deformation. Elongated break-up is especially significant for immiscible liquid-liquid dispersions (Zhou, 1997). The visual representation of droplet deformation types is shown in Figure 1-3.

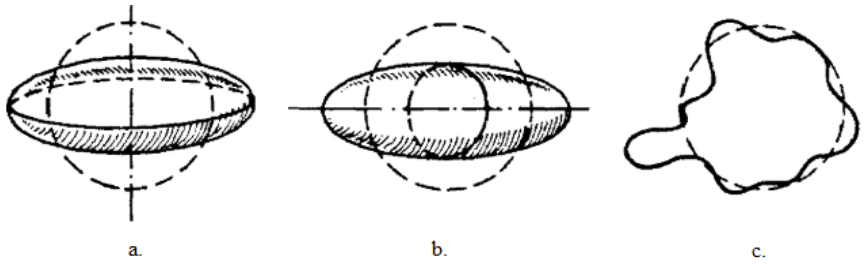

Figure 1-3: Types of deformation of droplets: a. lenticular, b. elongated, c. bulgy (from Hinze, 1955).

Ali et al. (1981) also revealed mechanisms for oil-water dispersions in stirred tank with PBT using a photographic method. They stated that two different mechanisms which are ligament and turbulent fragmentation play significant role in break-up of oil droplet. The ligament stretching mainly consist of two stages: first, the oil is stretched into ligaments or elongated sheets due to the velocity gradient between the vortex and the surrounding liquid and then, the ligament breaks into smaller droplets when the stretching becomes sufficient to form an unstable interfacial condition (Zhou, 1997). The ligament stretching mechanism is similar to the elongated breakup as Hinze (1955) defined. On the other hand, turbulent fragmentation mechanism occurs at higher Reynolds numbers (higher impeller speeds or low viscosity fluids). When large oil droplet enters directly into the vortex region near the impeller tip, a rapid deformation and break-up of oil droplet occurs without elongation. Calabrese (1979) also stated same mechanisms for dispersed phases which have high or low viscosity in stirred tanks. The representation of ligament stretching and turbulent fragmentation mechanisms are shown in Figure 1-4.

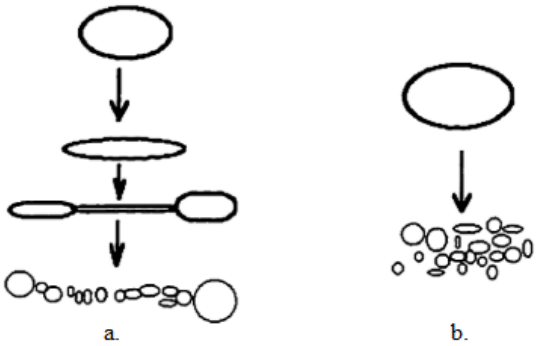

Figure 1-4: Representation of droplet breakage mechanism for oil-water dispersion: a. ligament stretching mechanism b. turbulent fragmentation mechanism (from Zhou, 1997).

Coalescence of droplets is also important mechanism for assessing the mixing performance. Coalescence is the combination of two or more droplets due to collision between suspended droplets in continuous phase. Coalescence occurs in two steps: collision and followed by film drainage. The film drainage step depends on the magnitude and duration of the force acting on the droplets. To break the separating film, a critical thickness should be in the range of 50 Å. For collision step, collision frequency is related to both agitation rate and the volume fraction of the dispersed phase. It is important to note that not all collisions cause the coalescence. When the contact time is short enough, critical thickness is not reached; thereby the droplets separate. The coalescence rate depends on the collision rate and the coalescence efficiency. The mobility of the liquid–liquid interface also affects the film drainage rate. Clean, mobile interfaces support efficient film drainage and lead to higher rate of coalescence (Leng & Calabrese, 2004).

In immiscible liquid-liquid dispersions, droplet generation and coalescence mechanisms strongly affect average droplet size and droplet size distribution. If coalescence mechanism is dominant in the system, the average droplet size gets bigger with time. However, droplet breakage and coalescence mechanisms may reach dynamic equilibrium; therefore, change in average droplet size cannot be observed after the equilibrium state (Pacek et al., 1999).

1.5 Role of Emulsifiers

Emulsification processes are used in various industries including the cosmetics, food processing, paint, petroleum, and pharmaceutical industries as explained before. Most emulsions are stabilized by the surfactants and global expected demand of surfactants was $30 billion in sales for 2017 (Tsabet & Fradette., 2015). Due to increasing demand of surfactants, less costly and greener alternatives such as solid particles attract the attention. In earlier decades, Ramsden (1903) and Pickering (1907) used solid particles to produce highly stable emulsions. In last decades, many studies focused on emulsion stability, type, size and rheological behavior of the emulsions. It was found that solid-stabilized (Pickering) emulsions are much more stable than surfactant-based emulsions due to their high adsorption energy (Binks., 2002). Solid particles have been utilized by many researchers that various types of inorganic particles such as silica, clay, and hydroxyapatite (Hap) and organic particles such as proteins, polysaccharides etc. can be effectively used as emulsifiers (Yang et al., 2017).

The representation of surfactants, and solid particles adsorption at oil-water interface is shown in Figure 1-5: Representation of adsorption with: a. surfactants, b. solid particles. The enhanced stability of Pickering emulsions is due to steric barrier around the droplets that is formed with close-packed network of particles. The particle interactions at a fluid interface is usually attributed to capillary forces (Levine et al., 1991, 1992, 1993). However, for surfactant-based emulsions, surfactants adsorb at the oil-water interface to prevent coalescence of the droplets by decreasing the interfacial tension between the phases.

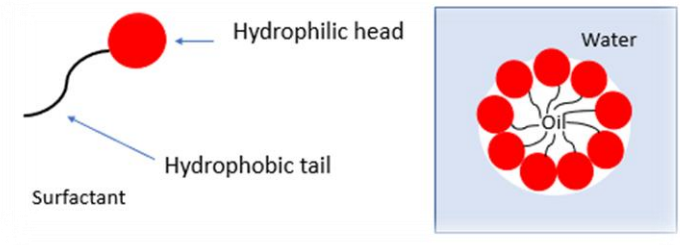

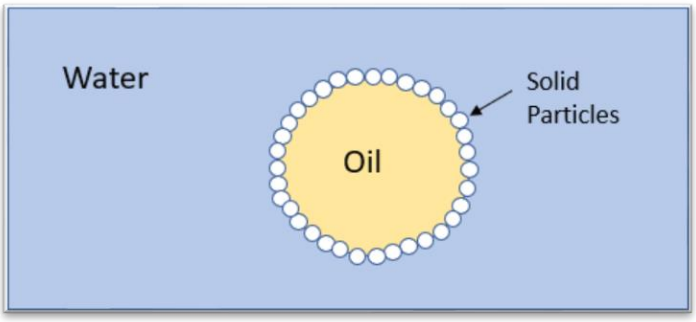

Figure 1-5: Representation of adsorption with: a. surfactants, b. solid particles.

During the emulsification with solid particles in a stirred tank, firstly the interface generation in high shear zone and then stabilization occurs, and partially covered and uncovered droplets will coalescence in coalescence zone; therefore final droplet size can be controlled by both capacity of interface generation and particle coverage as shown in Figure 1-6. However, with the surfactants, coverage step could be even faster than droplet breakage step since the surfactants lower the interfacial tension (Tadros, 2013; Tsabet & Fradette.,2015). This means that for surfactant-based emulsions droplet breakage and coverage steps do not have to occur respectively. Tsabet & Fradette (2015) also found that for Pickering emulsion production when low viscosity oils are used, the droplets are much smaller since the breakage process is more significant. In this study, low viscous silicone oil (100 cst) was used, and findings are evaluated in the light of this information.

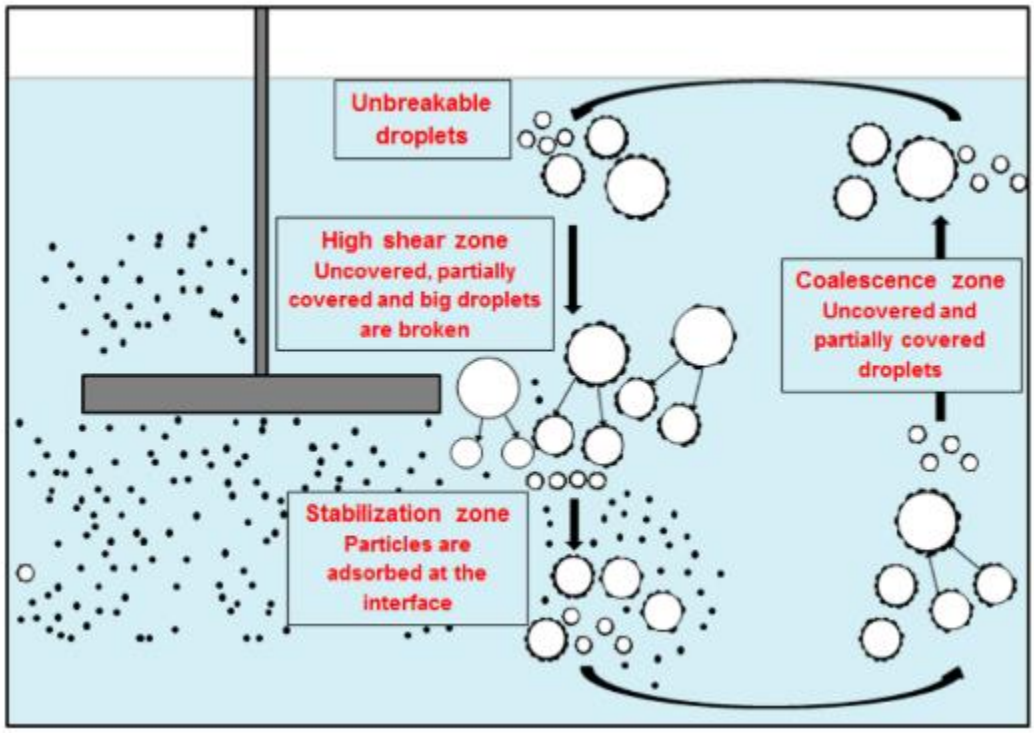

Figure 1-6: Representation of emulsification with solid particles in a stirred tank (from Tsabet & Fradette, 2015)

The enhanced stability of solid-stabilized emulsions is examined in two approaches. The first one is based on free energy analysis. It is stated that the stability is obtained when system reaches its minimal free energy. The detachment energy is given as following formula (Levine et al., 1989);

$$E = \pi R^2 \gamma_{ow} (1 \pm \cos\Theta)^2 \qquad (1.13)$$

The second approach is based on force analysis. This analysis can be examined in two steps: particle approach and adsorption. During particle approach (at shorter distances < 1 μm), it is showed that DLVO (Derjaguin, Landau, Verwey and Overbeek) forces: attractive Van Der Waals and repulsive electrostatic double layer forces, and non-DLVO forces: repulsive hydration and steric forces, attractive

hydrophobic forces are the main interactions (Tsabet, 2014). During the adsorption step, the stability is reached when the sum of the external forces which are the attractive gravity, capillary, hydrostatic pressure, and repulsive buoyancy and viscous forces is zero (Princen et al.,1967; Joseph et al., 2003). The force analysis showed the importance of capillary forces during adsorption mechanism (Princen et al.,1967).

Emulsion type by knowing properties of surfactant and solid particles are determined in different ways. For surfactant-based emulsions, hydrophobic and hydrophilic balance of the surfactant molecules is influential on the structure of the emulsion (oil in water-o/w or water in oil emulsions-w/o) (Tadros, 2013). For Pickering emulsions, solid particles are not amphiphilic as surfactants, but wetting conditions specify the type of emulsions: water-in-oil or water-in-oil emulsions. Wettability means the degree of wetting when the solid and liquid interact. This degree is defined as contact angle (Θ). The most stable emulsions are obtained using particles with intermediate hydrophobic properties (Θ~90°), whereas the least stable emulsions are obtained with highly hydrophobic (Θ>>90°) and highly hydrophilic particles (Θ<<90°) (Yan et al.,2001; Binks & Lumsdon, 2000). Emulsion type is controlled by particle affinity with both phases. For example, hydrophilic particles produce o/w emulsions and hydrophobic particles produces w/o emulsions as shown in Figure 1-7. This behavior is explained with the Bancroft rule: when the particles are initially dispersed in the phase that they have the most affinity, then this phase becomes the continuous phase. However, this behavior is only valid when volume of the dispersed phase is smaller than or equal to the continuous phase. Emulsion type can also be affected by oil polarity (Binks, 2002) and water pH (Yan & Masliyah, 1996) due their effects on particle wettability.

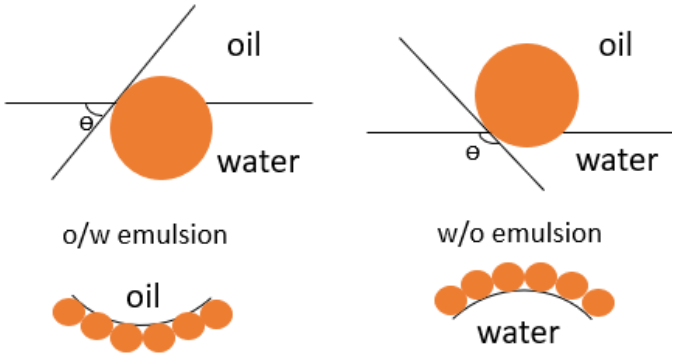

Figure 1-7: Representation of particle wettability (Adopted from Langevin et al., 2004).

Different parameters that affect emulsion stability have been revealed by many studies. Emulsions stability can be improved by increasing particle concentration (Arditty et al.,2003) which leads to a decrease in droplet size, reducing particle size (Binks & Lumsdon, 2001), using monodispersed (Tarimala & Dai, 2004) and ellipsoidal particles (Madivala et al., 2009) which is not easy to attain. It is also shown that high oil viscosities prevent stabilization by hindering particle adsorption (Golemanov et al., 2006). Apart from these studies, Tsabet & Fradette (2015) found that stabilization efficiency is increased with particle concentration until a certain limit since the mixing intensity decreases in the case of excess particle concentration. Also, it is indicated that the usage of high viscosity oils is also resulted in less efficient adsorption because it increases the adsorption time.

1.6 Relevant Studies for Emulsion Production in a Stirred Tank from Process Design Perspective

More work has been done on the emulsion stability, variety, size, rheological behavior of the emulsion than process design perspective. Only following studies explain the effect of the various parameters on the average droplet size from this perspective.

EL-Hamouz et al. (2009) studied the effect of dispersed phase addition point on the average droplet size with silicone oil-water and surfactant environment. It is argued

that at higher impeller speeds, the effect of dispersed phase addition point cannot be observed since first stage of droplet breakage mechanism, which is oil draw down into the impeller is not dominant as at lower impeller speeds. Also, it is indicated that tip speed is a better parameter for predicting droplet size than power per mass.

Emulsification processes are very sensitive to the continuous feeding time of the dispersed phase. Jahanzad et al. (2010) investigated the effect of addition time or feed rate of dispersed phase on type of inversion and the average droplet size for surfactant-based emulsions. However, phase inversion is undesirable in present study and therefore the study is evaluated only in terms of effect of dispersed phase addition time on average droplet size. It is indicated that lower addition time produces smaller droplets in case of phase inversion.

Manga et al. (2017) studied the effect of dispersed phase feed rate on droplet diameter with solid particles in case of stirred cell membrane emulsification. It is argued that when oil flux (oil feed rate) is decreased, smaller droplets are obtained since lower oil flux promotes the generation of new interfacial area.

The only pioneering work about some process parameters in a stirred tank for Pickering emulsions is conducted by Tsabet & Fradette (2015). In the study, emulsification experiments were conducted in an unbaffled stirred tank with an off-centered pitched-blade turbine. They investigated the effects of mixing time, emulsification time and impeller speed on the production of Pickering emulsions. Mixing and circulation times were measured with a decolorization technique for investigating the effect of impeller speed on the breakage and stabilization mechanism. It is shown that there is a strong interaction between the processing parameters and mixing tank hydrodynamics. Optimum increase in emulsification time and impeller speed decreases the average droplet diameter until the equilibrium. Further increase in both may causes adverse effect due to higher the particle/drop collision force under those conditions. Thus, the results of the study showed that the breakage and stabilization mechanism is strongly affected by shear level in the impeller zone, the energy dissipation rate, and circulation time of the fluid.

1.7 Motivation of Thesis

Pickering emulsions have more advantages over surfactant-based emulsions in terms of stability, biocompatibility, environmental risks and cost. In the literature, although there are extensive studies about effects of oil, water and solid particles properties on production of Pickering emulsions, there is a lack of information from a process design perspective with a stirred tank. Only the effect of two processing parameters which are emulsification time and impeller speed on the droplet size for Pickering emulsion production in a stirred tank have been investigated. This thesis aims to investigate another important processing parameter, which is feed rate of dispersed phase, that affects the droplet size for production of Pickering emulsions in a stirred tank, when the following hydrodynamic conditions were constant for all configurations: tip speed, power per mass and impeller Reynolds number. The comparison of these configurations at each of the hydrodynamic conditions provide information about not only whether the feed rate is an important parameter, but also whether it depends on emulsification time, the impeller type, size, feeding point and hydrodynamic conditions.

CHAPTER 2

EXPERIMENTAL PROCEDURE

2.1 Materials

Silicone oil (XIAMETER®, Dow Chemical) of 100 cSt viscosity at 25 ºC, 964 kg/m^3 density and 2.09x10^{-2} N/m surface tension, was used as dispersed phase. Distilled water was used as continuous phase. Interfacial tension between silicone oil and water is 60x10^{-3} N/m. It was measured by Attension® (Biolin Scientific). Hydrophilic calcite particles (TC-60®, MikronS) were used to produce oil-in-water (o/w) emulsions. Average particle size (d_{50}) is 17 μm. It was measured in Mastersizer® 3000 (Malvern) which is a particle size analyzer and density of these particles is 2700 kg/m^3. Microscope image of these grit shape particles is given in Figure 2-1.

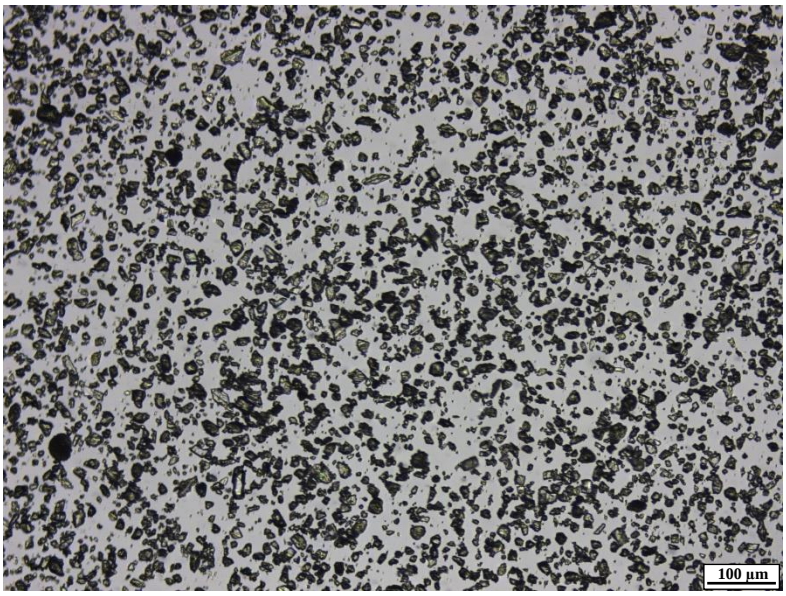

Figure 2-1: Microscope image of calcite particles in grit shape.

2.1.1 Viscosity Calculation for Silicone Oil-Water-Calcite Mixture

Dynamic viscosity of the silicone oil-water-calcite mixture is required to calculate impeller Reynolds number. Viscosity calculation of this system is conducted with the following equation which is developed by Roscoe (1952);

$$\eta_r = \frac{\mu_s}{\mu_c} = (1 - 1.35\Phi_s)^{-2.5} \quad (2.1)$$

where η_r, relative viscosity, μ_s, viscosity of suspension (dynamic viscosity of mixture), μ_c, viscosity of continuous fluid (0.00089 kg/ms) and Φ_s, volume fraction of calcite particles (3.3%). Thus, viscosity of the mixture is found as 0.000997 kg/ms from Equation 2.1.

2.2 Experimental Set-up and Methods

Emulsification experiments were conducted in a baffled stirred tank (1 L glass beaker) shown in Figure 2-2. The tank diameter (T) was 9.9 cm. Four evenly spaced baffles with a width (W) of T/10 were used.

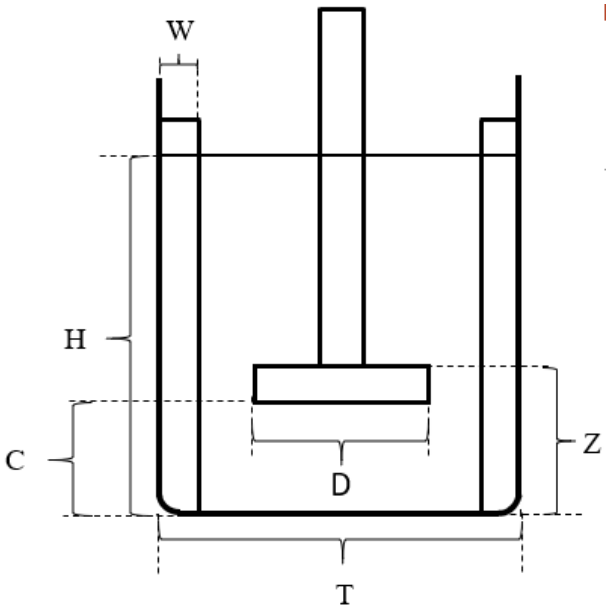

Figure 2-2: Schematic representation of the stirred tank.

Rushton Turbine (RT), 45° down-pumping pitched blade turbine (PBTD) and 45° up-pumping pitched blade turbine (PBTU) were used at two different sizes: T/2 and T/3. These impeller types are shown in Figure 2-3. The impeller was in the center of the tank and it was set to an off-bottom clearance (C) of T/3 for all experiments. The detail drawings of the impellers are given in Appendix A. The liquid height was equal to the tank diameter in all of the experiments. A mechanical stirrer (Daihan Scientific®) was used for agitation.

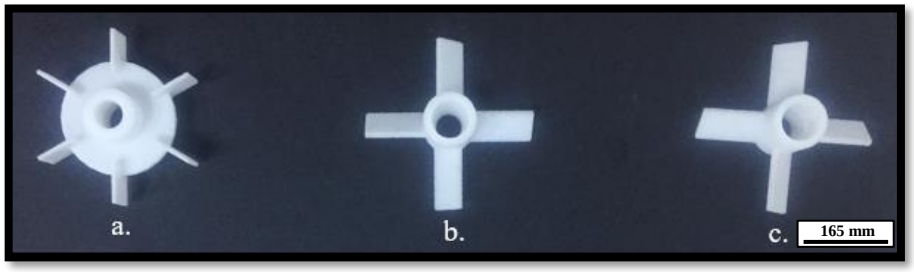

Figure 2-3: Images of 3D-printed impellers used in the experiments: a. RT, b. PBTU and c. PBTD.

The general experimental procedure is outlined below. In all experiments, first a certain amount of calcite particles - at a particle to oil ratio of 33 wt.% - were dispersed in water at a specified speed for 10 minutes to break up aggregates and to wet the entire surface of particles with water. Then, silicone oil was added to form an emulsion. The oil-to-water ratio was 43% (v/v). It was added either directly from the surface in 5 seconds using a graduated cylinder or by using the computer-controlled SEKO® peristaltic pump at specified feed time. Figure 2-4 shows the experimental set-up when the pump is used. Silicone oil was placed in a beaker which was located on an analytical balance (OHAUS®). The silicone oil was pumped into the tank through a feed tube (d_{feed}=5 mm) which is at a specified position. These positions were varied for each impeller type. The feed rate was set via a computer program which changes the electric motor voltage and the code is given in Appendix B. This change is based on the weight difference information that is supplied from the balance.

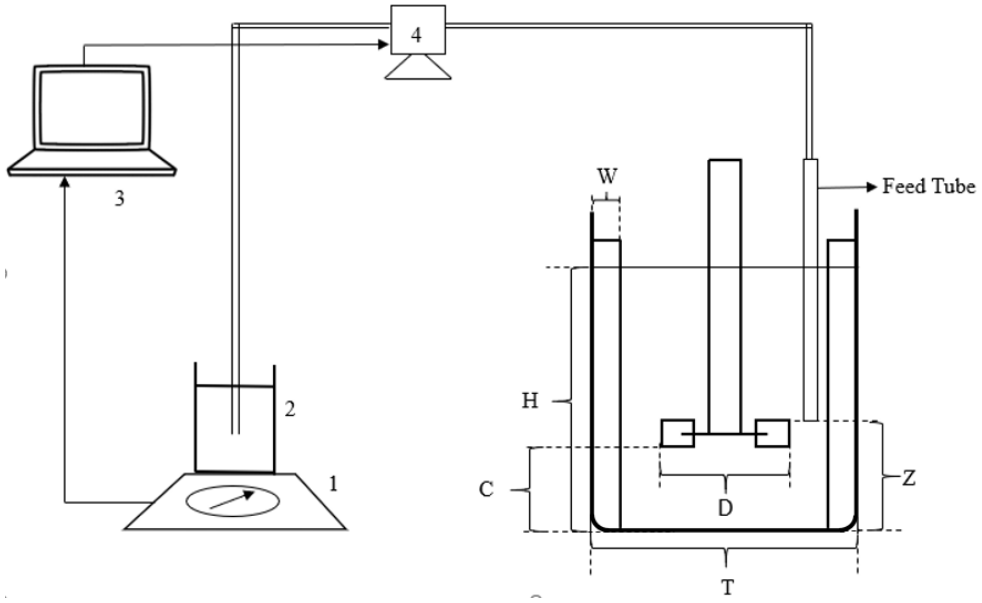

Figure 2-4: Schematic representation of experimental set-up. (1) OHAUS® analytical balance, (2) Silicone oil reservoir, (3) Computer, (4) SEKO® peristaltic pump.

The contents of the tank were stirred over a certain time. Then, the samples were taken using a small pipette to 20 ml vials. The droplet sizes were measured in MasterSizer 3000® (Malvern). The details of analysis methods are given in the following sections.

2.2.1 Feed Rate Controller

A peristaltic pump was used to feed the silicone oil at a specific rate. The feed rate of the pump was controlled instantaneously by measuring the weight of the reservoir. The controller aims to decrease the difference between the desired weight of the silicone oil fed into the tank (W_{set}) and actual weight of pumped oil that is measured at an instant ($W_{instantenous}$) to the stirred tank. The calculations are explained below.

First, the set weight (W_{set}) at any given time is calculated as follows,

$$W_{set}(t) = W_i - t.\dot{m}_{set} \qquad (2.2)$$

where $\dot{m}_{set}$ is set mass flow rate.

Second, instantaneous weight at any given time can be found by subtracting initial weight of the reservoir (W_i) from final weight (W_f):

$$W_{instantenous}(t) = W_i - W_f(t) \quad (2.3)$$

$$W_f(t) = t.\dot{m}_{actual} \quad (2.4)$$

where $\dot{m}_{actual}$ is actual mass flow rate that is measured at an instant.

The error is continuously calculated by the following equation until it is zero:

$$W_{instant\ error} = W_{set} - W_{instantenous} \quad (2.5)$$

Finally, the computer program adjusts the voltage according to the error.

The closed loop block diagram of the feed rate controller is shown in Figure 2-5. The output of the controller is the voltage that will be applied to electric motor of the pump (V_{motor}). The controller (ARDUINO®) changes the voltage with Pulse Width Modulation (PWM) technique. PWM is a method to get analog results using a digital source. Digital control is used to generate a square wave and a PWM signal can be switched between on and off (Timothy Hirzel, n.d.). Process transfer function (G_p) was used to describe the peristaltic pump. It relates the applied voltage and actual mass flow rate. For this transfer function, there is no need to use flow rate sensor because flow rate sensors on the market are not affordable in the case of very low flow rates. Instead of measuring flow rate via sensor, the balance can be used to measure the instantaneous weight.

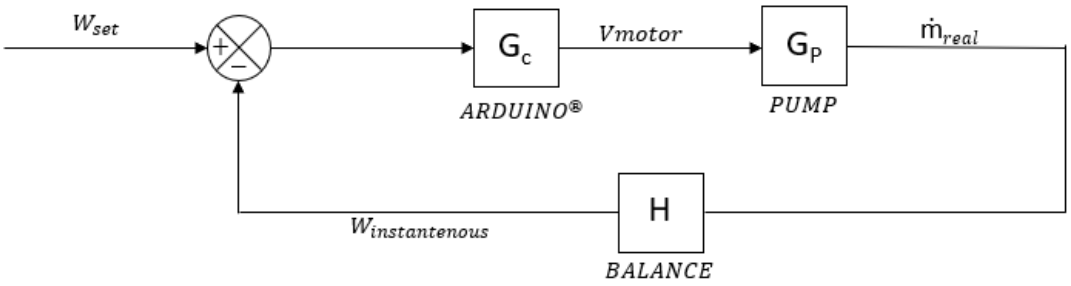

Figure 2-5: Closed loop block diagram of the feed rate controller. Transfer functions: G_c (Controller), G_p (Process) and H (Sensor/ Transmitter).

Besides of these, an interface software as shown in Figure 2-6 was created to insert the feed time and set flow rate easily.

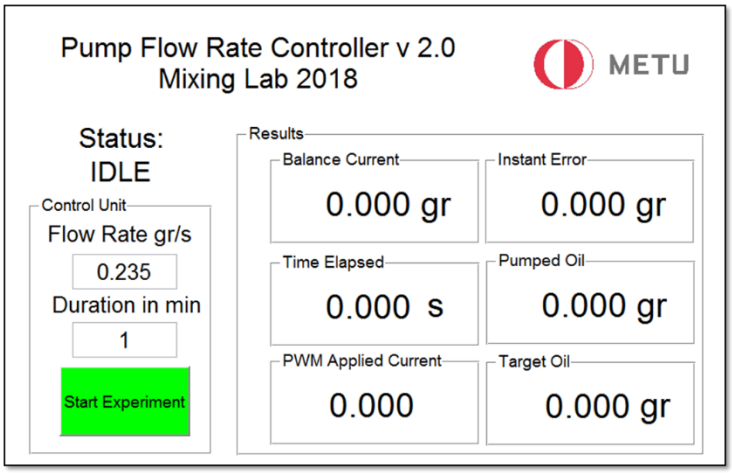

Figure 2-6: Image of the interface software.

2.2.2 Feed Positions

The position of the feed tube tip is important because local energy dissipation rate is very sensitive to position close to impeller (Assirelli et al., 2002). The point of maximum local energy dissipation changes with respect to the impeller type that is used. These points for the impellers under investigation are given in Section 1.2.5 based on literature information and are shown in Figure 2-7. The specific positions that are adapted to this system are listed in Table 2-1. Position 1 for PBTD, position 2 for RT and position 3 for PBTU indicate the highest energy dissipation points.

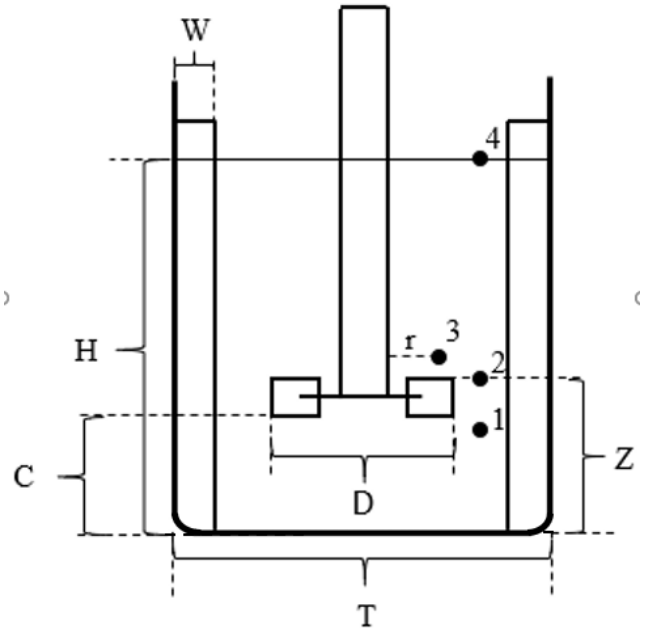

Figure 2-7: Feed positions.

Table 2-1: Geometrical details of the feed tube tip.

Feed Position	Position 1	Position 2	Position 3	Position 4
2r/D	0.97	0.97	0.55	0.97
z/H	0.28	0.36	0.42	1.0

The effect of the feed position on droplet size was tested for all these points with RT, PBTD and PBTU at two different sizes: T/2 and T/3. Since the position of the feed tube is critical, a lid was designed to keep the tube in precisely the correct radial position and to reduce the vibration and movement of the tube due to the forces around the rotating impeller to a minimum. In Figure 2-8, the tank covered with a lid can be seen.

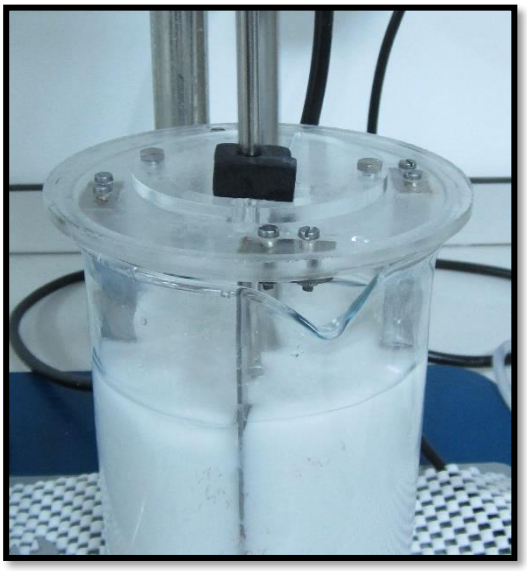

Figure 2-8: Image of the plexiglass lid fitted in 1 L stirred tank.

The lid design varied according to the sizes and the type of the impellers. The designs are shown in Figure 2-9. The round hole in the center of the lid seen in the figure helps positioning the shaft at the center of the tank.

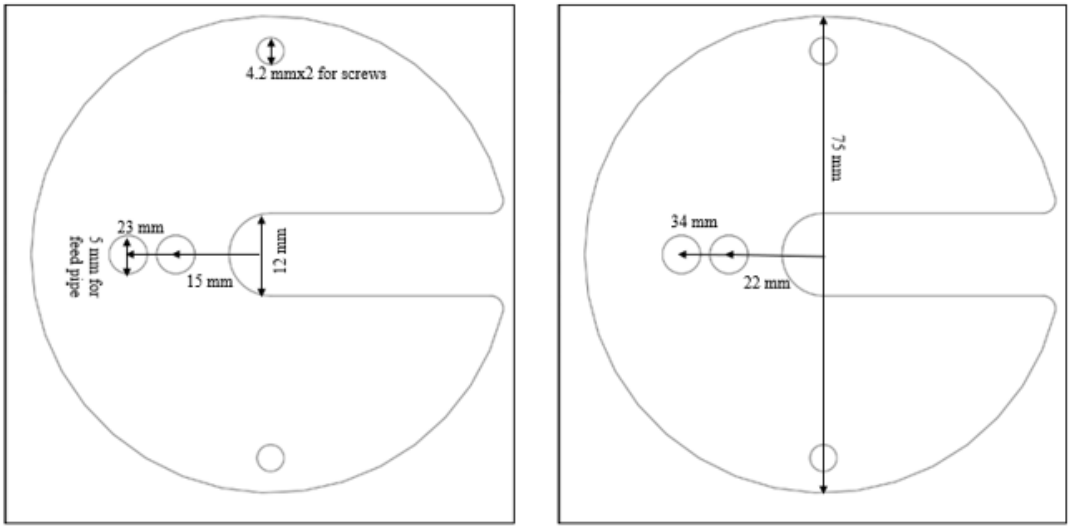

Figure 2-9: Drawings of different radial (2r/D) feed positions for T/2 and T/3 impellers as given in Figure 2-7: a. for position 3, b. for position 1, 2 and 4.

2.2.3 Optimization of Particle Concentration

Particle concentration was determined based on the amount of particles collected at the bottom of the tank at the end of the experiment. An average hydrodynamic condition (N=1000 rpm, emulsification time=2 h) was selected for the tests for to determine the necessary particle concentration. However, Tsabet & Fradette (2015) stated that adding much more particles results in decrease in the turbulent energy dissipation rate and in stabilization efficiency. Based on this, the tests were repeated until sufficient particles were observed in the continuous phase to stabilize the new interfacial area when the processing conditions are changed. Calcite concentration had been increased gradually (starting from 14 wt.% with 5 wt.% increase) until the sediment particles were observed at the bottom of the tank. Thereby, particle to oil ratio was decided as 33 wt.% at the end of the all tests.

2.2.4 Measurement of Size Distribution

The size distribution of the particles and oil droplets were determined by the laser light scattering method using MasterSizer 3000® (Malvern). Mastersizer can detect the particle size of wet samples (samples within a dispersant) within the 10nm-3.5mm range. Measurements were repeated twice for each sample. Emulsions were measured in half an hour after the emulsification to prevent coalescence and creaming effect. In this system, about 3-5 mL of the emulsion was added to Hydro Ev® liquid samples dispersion unit which was filled with 500 mL distilled water as a dispersant and they were stirred gently without breaking the droplets. Then, they were circulated continuously in the cell of MasterSizer 3000® (Malvern) during the measurements. Particle size distribution was presented as volume percentage vs. droplet diameter in the MasterSizer software. Volume size distribution is obtained by measuring the intensity of light scattered when a laser beam passes through a dispersed sample in the cell using Fraunhofer theory. Fraunhofer theory is known to work well for particles larger than 10 μm (Xu, 2000) .

In droplet size analysis, taking droplets without free particles from the vial is practically impossible. These free particles change the average droplet size significantly. In most of the particle and droplet size measurements, the distribution

was obtained as shown in Figure 2-10. In this figure, part a shows only calcite particle size distribution and part b shows size distribution of the droplets with free particle. Particle size distribution in part a overlaps free particle distribution in part b and a significant peak for droplets can be observed after the point where the free particle distribution ends up. For this reason, the smallest distribution was regarded as the size distribution of free particles in the emulsion and it was not considered in droplet size analysis. A similar method was followed by Tsabet & Fradette (2015) who also worked on Pickering emulsions.

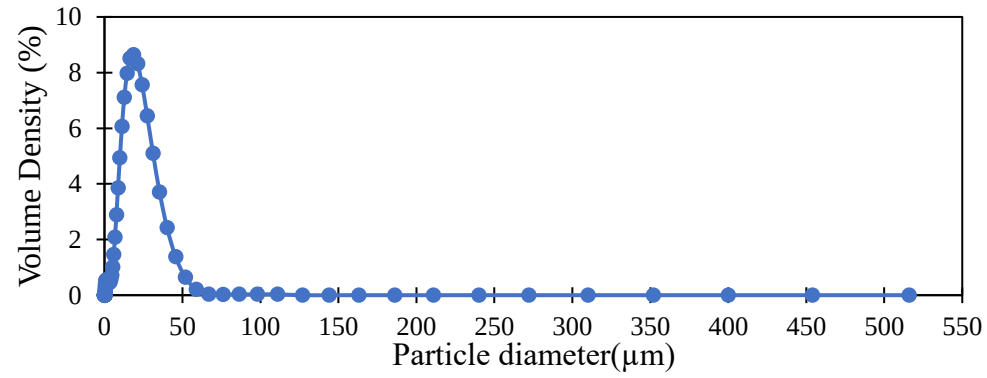

a.

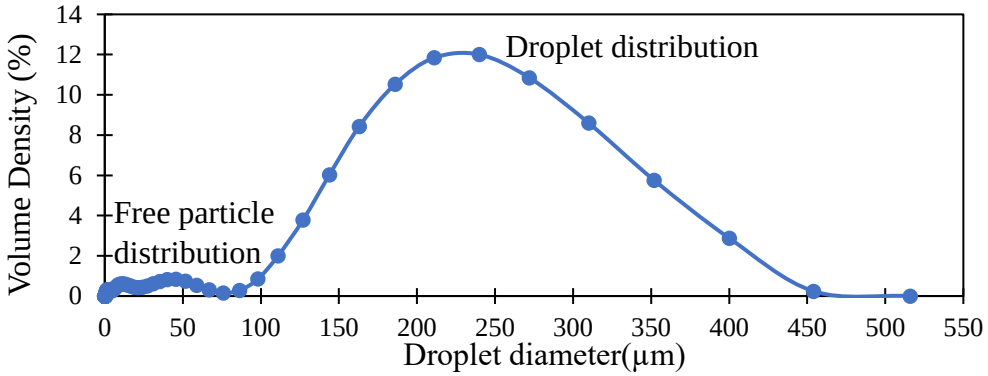

b.

Figure 2-10: Representative size distribution a. calcite particle, b. free calcite particles and oil droplets stabilized by calcite.

The size of the particles and oil droplets were measured in terms of d_{10}, d_{50}, d_{90}, d_{43} and d_{32}. Average particle size is often defined in terms of d_{50} if particles are in narrow range. For the measurement of average droplet size, droplets are often represented in

terms of d_{32} or d_{43}. d_{32} is a marker of surface area and smaller droplets which have high surface area effects this value but d_{43} can measure small amounts of flocculation or coalescence in a polydisperse emulsion with volume-based consideration (Larsson & Friberg, 1990). So, by considering polydisperse emulsions that were obtained in this study, the average size of oil droplets was expressed in terms of d_{43}. To clarify d_{32} and d_{43} difference, values of them from one of the representative experiments are shown in Figure 2-11.

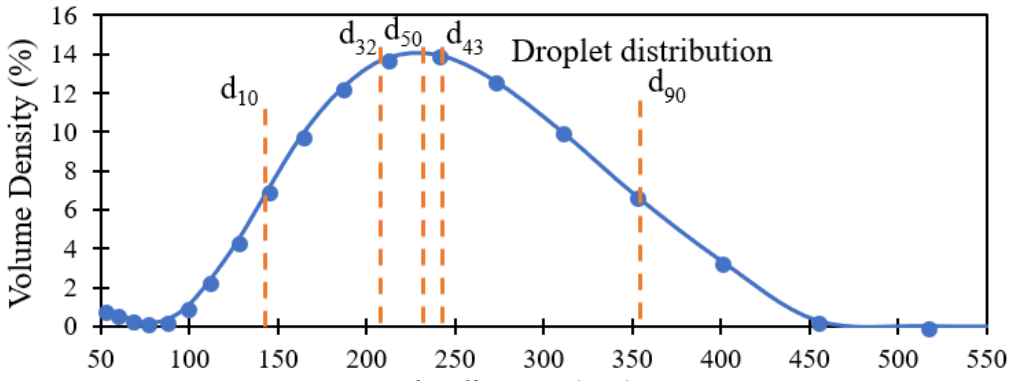

Figure 2-11: Representation of d_{10}, d_{32}, d_{50}, d_{43} and d_{90} values.

The width of droplet size distribution is also given as span of distribution. It can be calculated from following formula:

$$\text{Span} = \frac{[d_{90} - d_{10}]}{d_{50}} \tag{2.6}$$

In this formula, d_{10}, d_{50}, and d_{90} are diameters at 10%, 50%, and 90% cumulative volume, respectively. In other words, $[d_{90} - d_{10}]$ is the width of the data and d_{50} is the median diameter (Mahdi Jafari et al., 2006).

Microscope image of the representative droplets is presented in Figure 2-12.

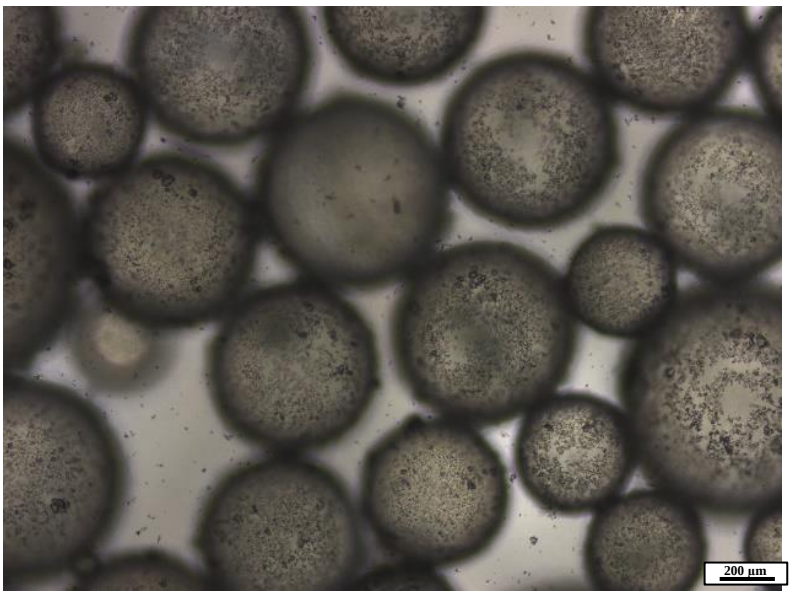

Figure 2-12: Microscope image of the droplets stabilized by calcite particles.

CHAPTER 3

RESULTS AND DISCUSSION

To investigate the effect of feed rate on average droplet size at different hydrodynamic parameters, first the time required for emulsifying the mixture and then proper feeding point for each impeller type were determined. Then, the change in average droplet size was investigated by varying the feed rate at a constant value of each of the selected hydrodynamic parameters: tip speed, power per mass and impeller Reynolds number. The span of droplet size data is also reported where span=0 is a representation of perfectly monodispersed droplets.

3.1 Effect of Emulsification Time on the Average Droplet Size

During the emulsification process, first interface is generated by droplet breakage, then particles are adsorbed on oil-water interface (Tsabet & Fradette, 2015). The adsorbed particles form a steric barrier which stabilizes the droplets. Partially covered and uncovered droplets may coalesce later until a dynamic equilibrium state is reached. In this section, the effect of emulsification time on the average droplet size was investigated to determine the emulsification time at which a (near) dynamic equilibrium is reached. The experiments were done at constant tip speed (V_{tip}) of 3.11 m/s and the emulsification process was observed over 4 hours.

In Figure 3-1a, the effect of emulsification time on the droplet size for different impellers is shown. No significant change over 4 hours of emulsification is observed except for RT-T/2 and PBTU-T/2. For the RT-T/2, the average droplet size differs 10% between 30 minutes and 2 hours, but it remains constant afterwards until the end of the fourth hour. For the PBTU-T/2, the maximum difference in average droplet size is observed between 2^{nd} and 3^{rd} hours as 5%, which can be considered as quite small. The results show that for all configurations, beginning from 2 hours of emulsification time the average droplet size does not change. This is because an

equilibrium between interface generation, stabilization and coalescence is reached. Based on this, for the rest of the experiments, emulsification time was set as 2 hours. In Figure 3-1a, the effect of impeller type and size can also be compared according to the average droplet sizes. The average droplet sizes are listed in decreasing order as the following: PBTU>PBTD>RT. Also, under these conditions the impeller size matters only for PBTU due to its upward flow pattern which is explained in detail in Section 3.3.1.

In Figure 3-1b, the effect of emulsification time on span of distribution is shown. For PBTU and RT, T/3 impellers have a narrower distribution compared to the other impellers, and their span are not affected from the emulsification time. PBTD-T/3 has a wider span initially but beginning from the 2nd hour it overlaps with the other T/3 impellers. For T/2 impellers, span of distribution for different types of impellers are almost the same except for the 3rd hour. This shows that the selection of 2 hours as the emulsification time is acceptable for both T/3 and T/2 impellers.

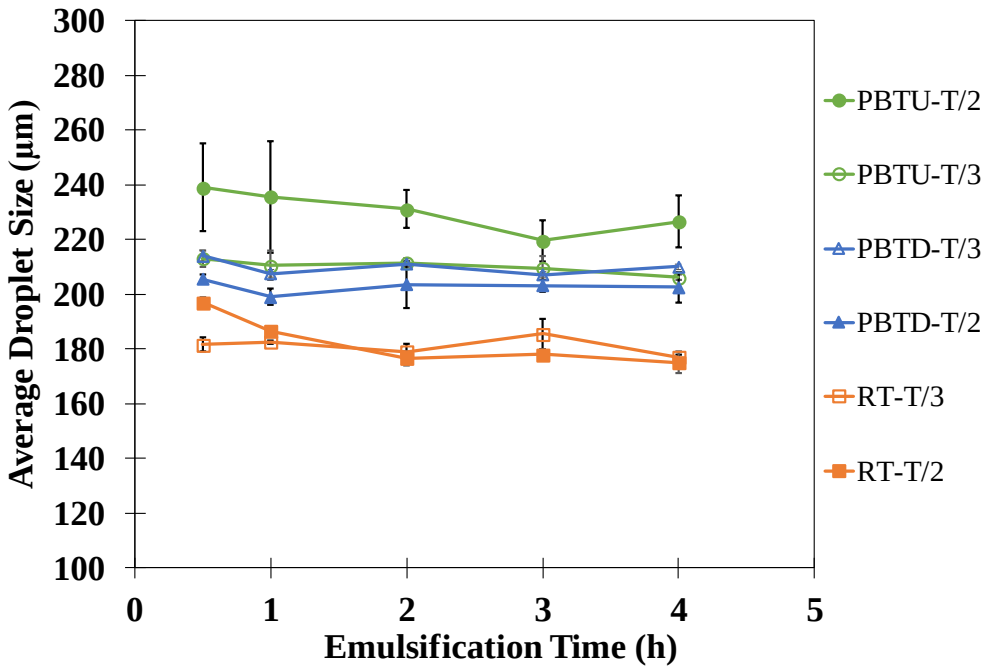

a.

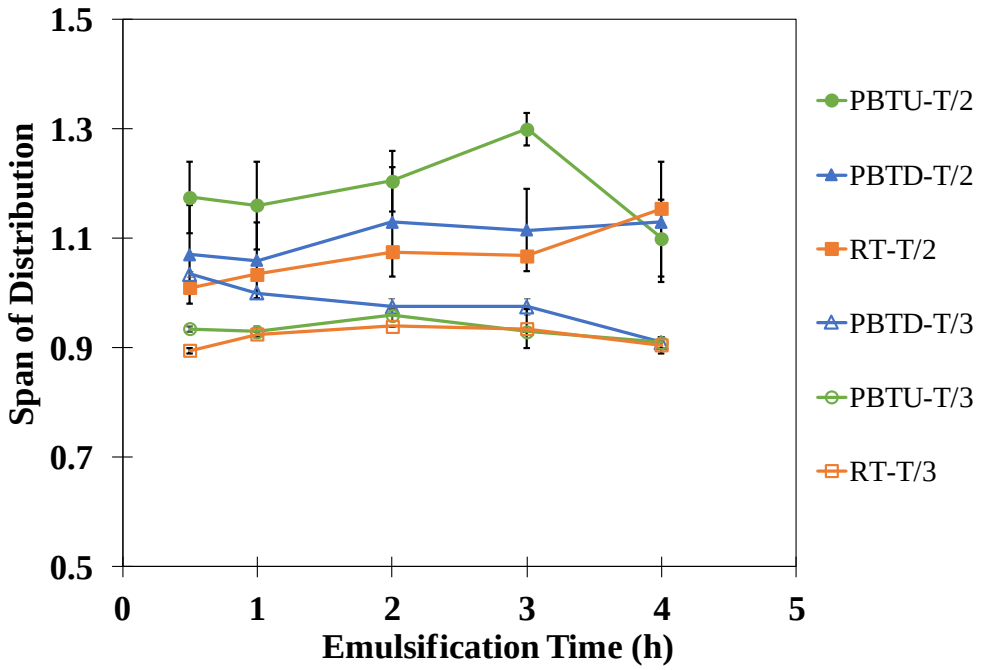

b.

Figure 3-1: The effect of emulsification time on a. the average droplet size b. span of distribution.

3.2 Effect of Feed Position on the Average Droplet Size

In this section, the effect of feed position on the average droplet size and span of distribution are investigated for RT, PBTD and PBTU impellers of T/2 sizes. Davies (1985) stated that average droplet size is related to energy dissipation rates and higher energy dissipation rates produce smaller average droplet sizes. Based on this, in Figure 3-2a, silicone oil was fed from different feed positions that were listed in Table 2-1. These positions were determined based on the literature as mentioned in Section 1.2.5. The positions are the highest energy dissipation points for each of the impellers to be able to observe the minimum average droplet sizes that can be obtained. The power per mass is constant for all impellers at 243 W/kg and silicone oil was fed in 900 s. The data agrees with Davies' (1985) findings: the minimum average droplet size for each impeller is achieved at the point of highest energy dissipation. These points are z/H = 0.28, 0.36 and 0.42 for PBTD, RT and PBTU, respectively.

The oil was fed from these highest energy dissipation points in the rest of the experiments. It should, however, be noted that the average droplet sizes change only slightly between the highest energy dissipation point and the surface feed point under these conditions. This indicates that if feed rate is varied, only the effect of feed rate on average droplet size can be observed whether the oil is fed from the surface or impeller zone at these conditions. This observation may be related to the high mixing intensity, which allows the system to reach equilibrium quickly.

In Figure 3-2b, effect of feed position on span of distribution is given. The span of PBTU and PBTD are not affected from the feed position; however, this is not the case for the RT. The span varies significantly depending on the feed position. The smallest span of distribution is obtained at the highest energy dissipation point which agrees with the findings of Figure 3-2a.

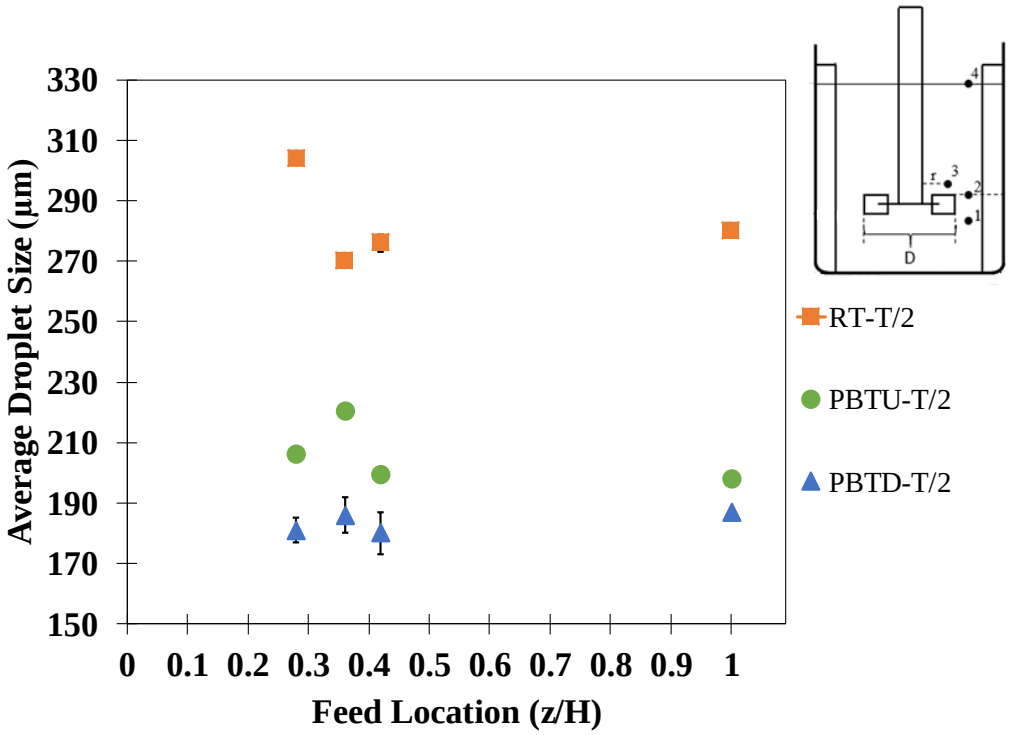

a.

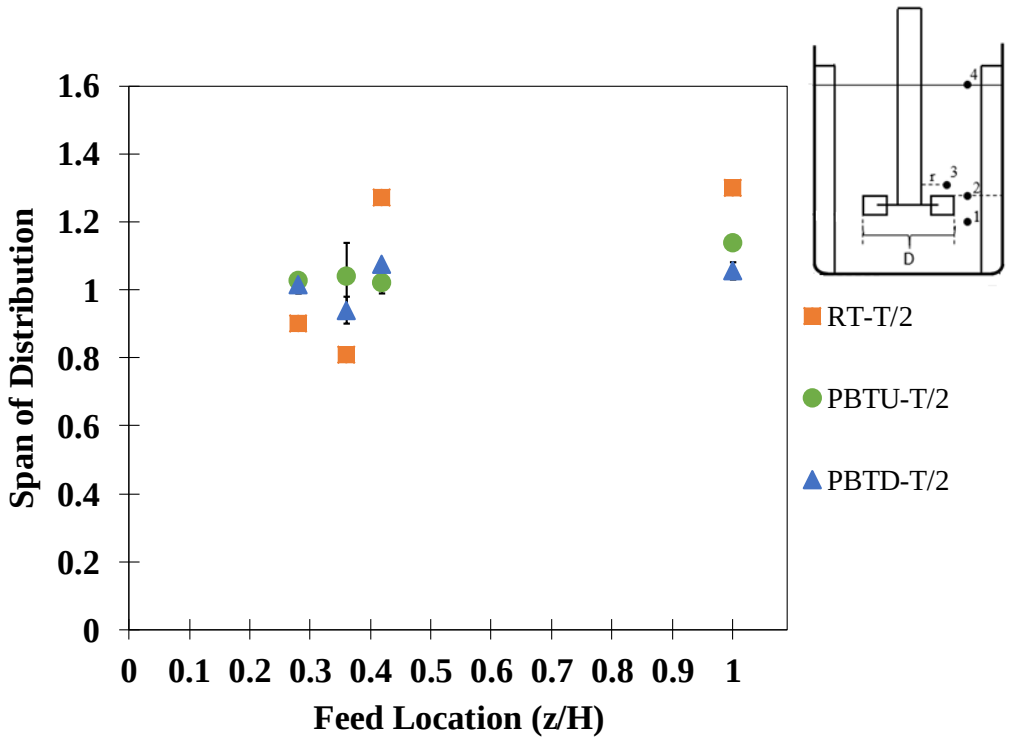

b.

Figure 3-2: Effect of feed position on a. the average droplet size b. span of distribution for RT, PBTU and PBTD, T/2 at constant PPM=243 W/kg, 900 s feed.

3.3 Effect of Feed Rate on Average Droplet Size at Constant Hydrodynamic Parameters

Up to this point, the emulsification time and feed positions for each impeller were determined. In this part of the study, the silicone oil was fed either in 5 s from the surface or in 900 s from the point of the highest energy dissipation for each impeller. It should be noted that although feed position appears to be another parameter besides the feed rate, only the effect of feed rate is observed between 5 s and 900 s feeding due to the insignificant difference in droplet size at the two feeding positions as explained in Section 3.2. Effect of feed rate on the average droplet size and span of distribution were investigated at a constant value of each of the following hydrodynamic parameters: tip speed, power per mass and impeller Reynolds number. Since the maximum local energy dissipation rate is related to both tip speed and power per mass from Equations (1.11) and (1.12) for predicting the average droplet size, the results are interpreted in the light of this. The findings are associated with the literature findings which may occur in surfactant-based or only liquid-liquid

dispersion systems rather than Pickering emulsions environment throughout this chapter. In the text, the effect of feeding is evaluated in terms of feed rate or feed time. In the figures feed time is used for representing the data. In all the experiments a total of 534 ml of silicone oil was added over a certain feed time, the ratio of which gives the feed rate.

3.3.1 Constant Tip Speed

In Figure 3-3a, the effect of feed rate on the average droplet size at constant V_{tip} of 3.11 m/s for six impellers is shown. The data also allows for a comparison of average droplet sizes obtained at two feed rates with six impellers. This aspect is evaluated first.

Impellers can be sorted according to the average droplet size they yield in decreasing order as the following: PBTU>PBTD>RT. The upward flow produced by PBTU has a negative impact on dispersing the oil phase. The discharge of the impeller flows up towards the surface. The oil tends to stay in the upper part of the tank due to its smaller density. This upper part is also the coalescence zone. Thereby, circulation time of PBTU can be higher compared to the other impellers that lead uncovered droplets stay longer in the more quiescent regions. This behavior can be associated with the findings of Zhao (2011) who also found that PBTU has longer mixing time among RT and PBTD for liquid-liquid dispersions at constant tip speed. Consequently, the poor dispersion of oil phase produces larger drops compared to the other impellers. The smallest average droplet size is obtained with the RT. This can be due to the intense energy dissipated around the impeller with the RT, which is different than the other impellers. As a result, the droplets formed are more rigid and coalesce much less, allowing the equilibrium to be reached rapidly.

When the droplets obtained with the same type of impeller, but two different sizes, it is seen that for PBTD and RT the change of impeller diameter does not affect the average droplet size; however, PBTU-T/3 produces smaller average droplet size compared to PBTU-T/2. This can be related to the poor dispersion of oil phase with PBTU-T/2 impeller due to the flow pattern. When the impeller tip speed is kept constant but diameter is decreased from T/2 to T/3 the impeller speed – therefore the

energy input- increases. This helps overcoming the disadvantage of the flow pattern of the PBTU impeller at T/3 size and the average drop size decreases.

Figure 3-3a shows that the average droplet sizes obtained with both sizes of RT and PBTU, and with PBTD-T/2 are not affected by the feed time. For these impellers under these conditions, turbulent fragmentation dominates; thereby equilibrium time is decreased. Higher energy input of these impellers leads to faster initial breakage and stabilization of droplets; therefore, smaller and rigid initial droplets are produced. Because of this, the effect of the feed rate cannot be observed in 900 s. However, only with PBTD-T/3, if the feed time is increased to 900 s, the minimum average droplet size is reduced by 11%. This is surprising as the energy input of PBTD-T/3 is higher than PBTD-T/2 at the same tip speed and the minimum average droplet size should have been reached with the T/3 impeller if it has already been reached with the T/2 impeller. It is clear that level of energy input (power per mass) is not sufficient to describe the droplet breakage and stabilization performance among different impellers. This is possibly due to the complex interactions between the breakage, coalescence and particle adsorption mechanisms during stabilization of Pickering emulsions as pointed out by Tsabet & Fradette (2015). The higher energy input increases particle-droplet collision frequency and efficiency for PBTD-T/3 which possibly improves the particle attachment process. This would mean that the newly formed interphase is effectively covered by the particles, leading to a smaller average droplet size.

The corresponding effect of the feed rate on span of distribution is given in Figure 3-3b. The span of distribution for PBTU-T/2, RT-T/2 and RT-T/3 was not affected from the feed rate. PBTU-T/3 and PBTD-T/3 have a slight increase indicating a wider droplet size distribution with the 900 s feed. Even average droplet size of PBTD-T/2 was not affected from the feed rate as shown in Figure 3-3a but the span is narrower when the feed is added in 900 s. When comparing the width of distribution for all impellers, RT-T/3 provide the narrowest distribution among the impellers. This observation analogous with experimental results of Podgórska (2009) in the liquid-liquid system without any surfactants: PBT in both up and down pumping modes

gives wider distribution than RT at constant tip speed because of lower level of energy input.

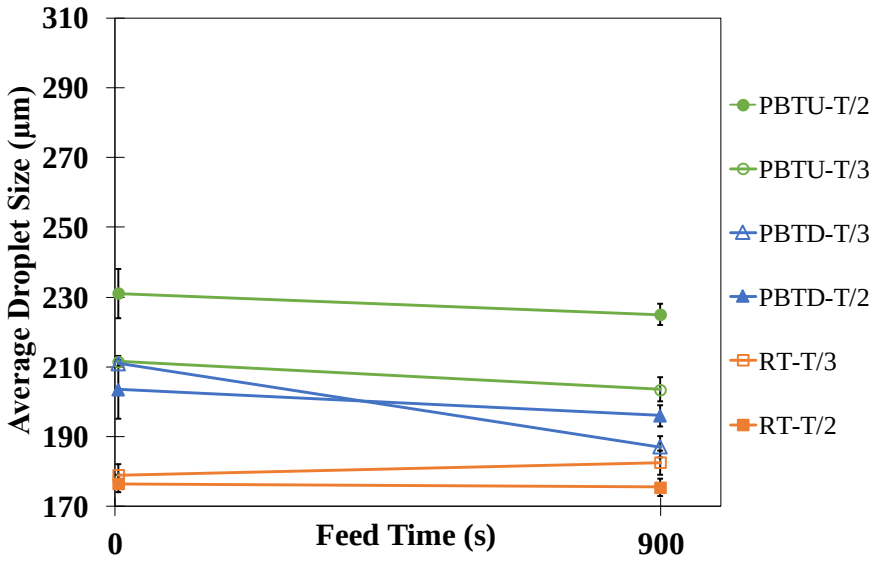

a.

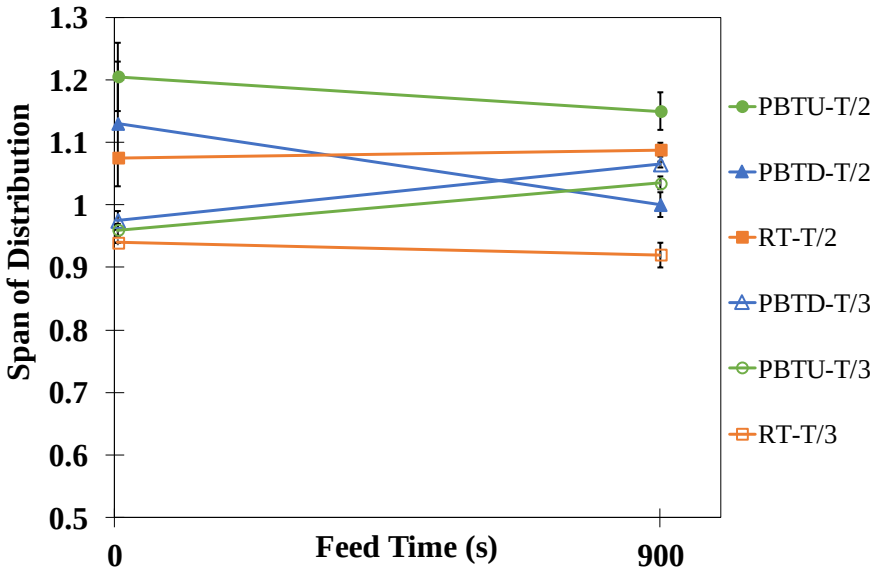

b.

Figure 3-3: Effect of feed rate on a. the average droplet size b. span of distribution at constant V_{tip}=3.11 m/s.

3.3.2 Constant Power Per Mass

Power consumption is an important parameter in designing stirred tanks for most applications. The energy provided by the impeller to the fluid is the source of any fluid motion, and it is often considered as a determining factor for product properties. A rough estimation of this energy is done by dividing the power consumption by the impeller swept volume. This is called power per mass (PPM).

The effect of feed rate on the average droplet size is investigated for six impellers at the same PPM of 243 W/kg. The results are given in Figure 3-4a. The average droplet size is not affected from the oil feed time with both sizes of PBTU and T/2 size of PBTD. However, the average droplet sizes are reduced by 7%, 12% and 11% with RT-T/2, RT-T/3 and PBTD-T/3 respectively when the feed time is increased from 5 s to 900 s. This is because newly generated droplets are smaller and covered quickly by particles in longer feed times.

PBTD-T/3 data is exactly the same as the data given in Figure 3-3a; therefore, it was expected to observe an effect of feed time on the droplet size. RT however, shows a different behavior this time. A comparison of tip speeds is required to explain this behavior since the average droplet size is related to maximum energy dissipation rate, and maximum energy dissipation rate is based on the impeller speed and power at the same time. At the same power per mass, RT has lower tip speed compared to PBT impellers. At lower tip speed, the minimum average droplet size is not achieved rapidly. This indicates that the effect of feed rate can easily be observed in lower tip speeds.

The effect of impeller size and type on the average droplet size are also studied at same power per mass. For 5 s of oil addition, T/2 impellers produce smaller average droplet size compared to T/3 impellers. This may be caused by stronger circulation of T/2 impellers. A stronger circulation means smaller circulation time for all T/2 impellers. When circulation time decreases, the droplets move into the impeller zone more frequently, improving the interface generation. This yields smaller average droplet sizes. Within each impeller type, the average droplet size is the same for both sizes when the oil addition time is 900 s. This means that for these impellers the new

dynamics introduced by feeding the oil slowly cancels out the faster circulation dynamics and the effect of impeller diameter is removed.

When the average droplet sizes are compared according to impeller type, it is seen that the RT produces the largest average droplet size and PBTD yields the smallest average droplet size at constant power per mass. Under these conditions, it is concluded that among different impeller types smaller droplets are obtained by low power impellers which are PBTU and PBTD at both sizes: T/2 and T/3. This agrees with the study of Pacek et al. (1999) which is conducted in surfactant free liquid-liquid system with low viscosity dispersed phase, Podgórska (2009) and EL-Hamouz et al. (2009) which were conducted in liquid-liquid system with surfactant and low viscosity dispersed phase. It is explained that PBT has higher tip speed (or energy dissipation rates) in the impeller zone at constant power per mass. Pacek et al. (1999) also argued that low power impellers produce smaller average droplet size due to having shorter circulation time under same conditions. The similar behaviour in the case of Pickering emulsions in Figure 3-4a can be explained with higher tip speed and shorter circulation time which may increase both interface generation and particle-droplet collision frequency thus improving the stabilization mechanism. Finally, PBTU produces larger average droplet size than PBTD due to longer circulation time as was explained in previous section.

In Figure 3-4b, it is seen that the span of distributions is not affected from the feed rate for these conditions. RT-T/3 produces the narrowest distribution among all impellers. Wider distributions are obtained with T/2 impellers. RT-T/2 has the widest distribution since the tip speed is very low compared to other impellers at this constant power per mass. Span factor of PBTD is not affected from the size.

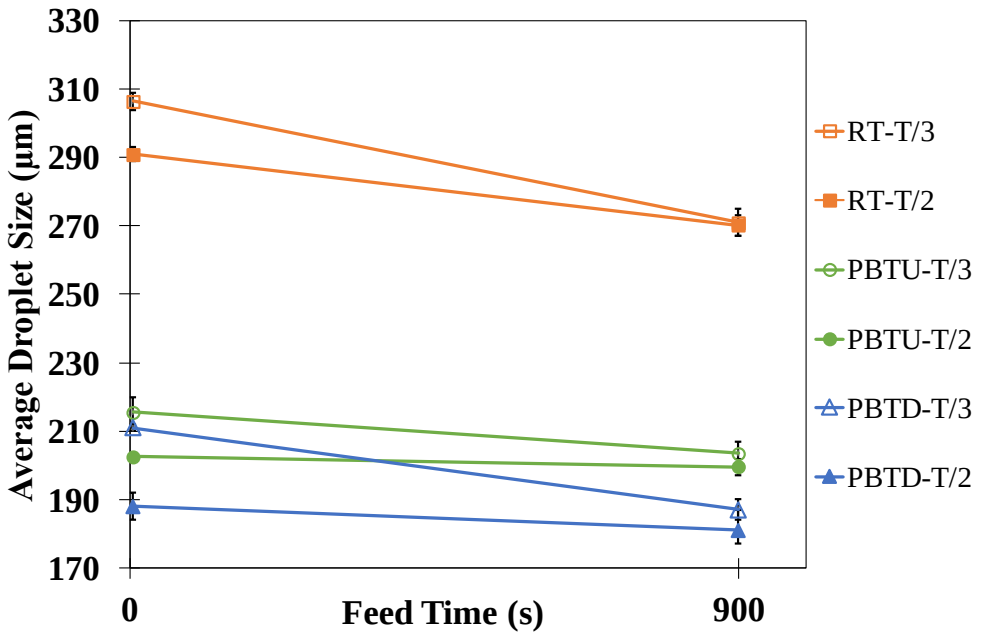

a.

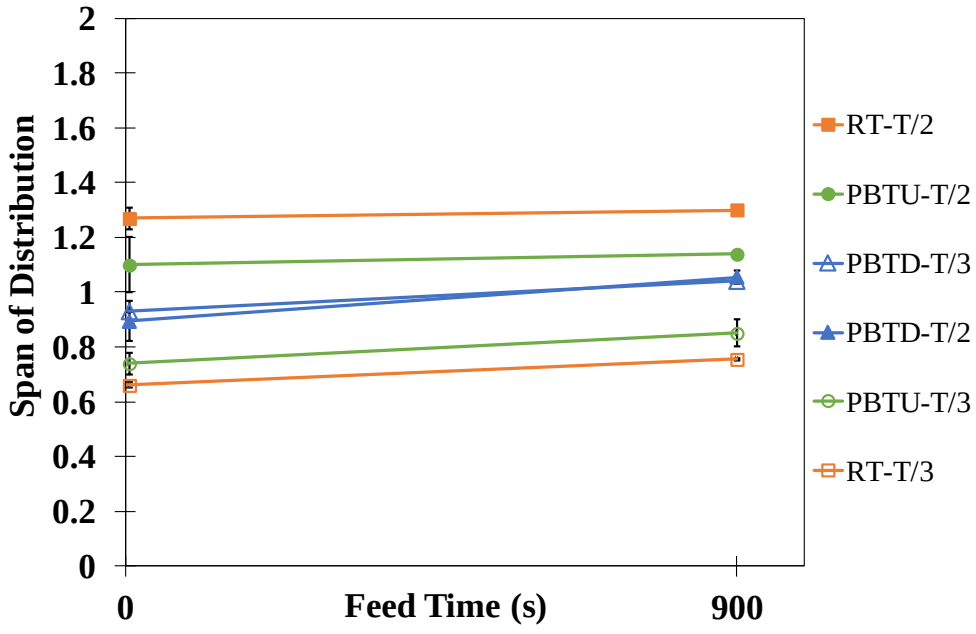

b.

Figure 3-4: Effect of feed rate on a. the average droplet size b. span of distribution at constant PPM=243 W/kg.

3.3.3 Constant Impeller Reynolds Number

Impeller Reynolds number is one of the important design parameters that characterize flow in the tank. The influence of feed rate on the average droplet size is investigated at constant impeller Reynolds number of $3.3x10^4$ which indicates fully turbulent regime. The data is given in Figure 3-5a. For PBTD-T/3, the average droplet size decreases by 11% when the oil feed time is increased from 5 s to 900 s. For PBTU-T/2, PBTU-T/3 and RT-T/2 the average droplet size is affected only slightly (4%) by the feed rate. Decreasing feed rate produces smaller droplets as explained earlier in Section 3.3.1 and 3.3.2 for particular impellers. The reason that some impellers do not get affected from the feed rate can be potentially explained by an equilibrium between interface generation and particle adsorption mechanism.

The effect of impeller size and type on the average droplet size are also investigated at constant impeller Reynolds number. Under these conditions, T/3 impellers produce smaller average droplet size since they have much higher tip speed and dissipation energy compared to T/2 impellers. For both sizes of impellers, the general trend of the average droplet size obtained with different impellers in decreasing order is the following: PBTU, PBTD and RT. The order was the same for the data at constant tip speed in Section 3.3.1.

In Figure 3-5a, there is a significant gap in average droplet size between T/2 and T/3 impellers at constant impeller Reynolds number. When, the data for only T/2 and T/3 is considered; however, it can be seen that the average droplet sizes are close to each other for all three impeller types. Fixed impeller Reynolds number and fixed impeller diameter correspond to constant tip speed. As seen in Section 3.3.1, the average droplet sizes are close to each other for all impeller types and sizes at constant tip speed. This indicates that tip speed is a better parameter to relate average droplet size to hydrodynamics among various impellers. The smallest droplet size is obtained with RT-T/3 due to its higher tip speed and shear level.

The effect of feed rate on span of distribution at constant Reynolds number is shown in Figure 3-5b. The width of distribution is narrower for T/3 impellers due to their higher level of energy input. All T/2 impellers yield the same span of distribution.

The narrowest distribution is obtained with RT-T/3. For PBTU-T/3 and both sizes of PBTD, the span factors are slightly affected by the feed rate: lower feed rate results in wider distribution.

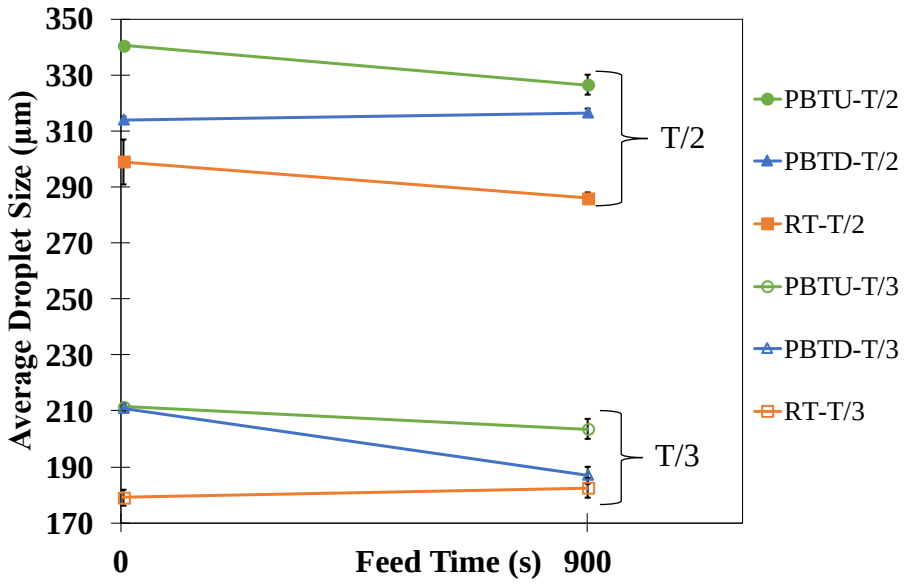

a.

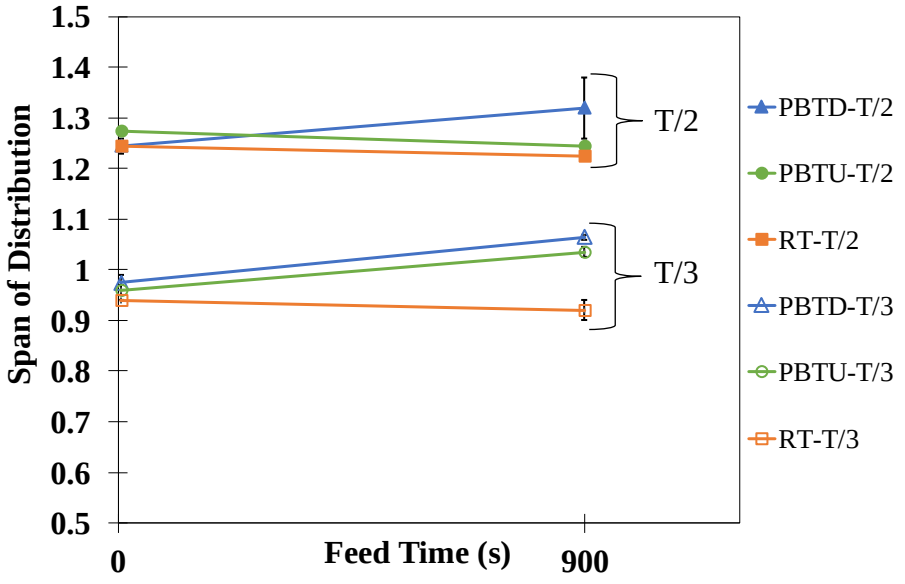

b.

Figure 3-5: Effect of feed rate on a. the average droplet size b. span of distribution at constant Re = 3.3×10^4.

3.3.4 Comparison of Different Hydrodynamic Parameters

In this study three different hydrodynamic parameters were considered for Pickering emulsion production: tip speed, power per mass and impeller Reynolds number. At constant tip speed, RT produces smaller average droplet size since it has higher shear level around the impeller compared to PBT. The average droplet sizes among all impeller type and sizes are close to each other at constant tip speed. This indicates that tip speed is a good candidate for design. However, power per mass is proportional to tip speed and power consumption is important in comparing the performances of different impellers. If the concern is power consumption, it is better to select the impeller that provides the smallest droplet size at the same power per mass among the three tested. This impeller is the low power impeller, PBTD, rather than RT.
The other parameter is impeller Reynolds number. The least favourable parameter to relate average droplet size is impeller Reynolds number because the gap in average droplet size between T/2 and T/3 impellers is tremendous at constant Reynolds number compared to the other parameters. However, at constant impeller Reynolds number, equal diameter impellers produce similar average droplet sizes. This is also related to the tip speed because at a fixed impeller Reynolds number, the tip speeds are the same for the equal size impellers. Also, at constant impeller Reynolds number, T/3 impellers produce smaller average droplet sizes due to higher tip speed compared to T/2 impellers.

This analysis shows that tip speed is the best parameter to compare the impellers; however, the other two parameters also have their advantages in design of stirred tanks and they are related to the tip speed in different forms. This indicates that these parameters should not be fully ignored in design.

3.4 Effect of Feed Rate at Different Impeller Speeds on the Average Droplet Size for Various Impellers

Tip speed was found to be the important parameter in comparing different impeller types. Tip speed is directly related to the impeller speed and impeller diameter. In this section, the influence of feed rate on the average droplet size at various impeller speeds for the T/2 impellers is investigated.

The data of RT-T/2 is presented in Figure 3-6a. For the lower impeller speeds, a decrease of 4% and 7% are observed at 785 rpm and 850 rpm, respectively. At both speeds, when the oil is fed in 900 seconds, the newly generated droplets obtained are smaller compared to feeding in 5 seconds. This new interphase is quickly covered by particles and smaller average droplet sizes are obtained at the end of the process. At 1200 rpm; however, the first droplets that are formed are most likely in similar sizes at both feed times due to higher tip speed and shear, and the final average droplet sizes do not change. The emulsion reaches equilibrium rapidly at higher impeller speeds, and more slowly at lower speeds leading to a visible effect of feed rate on the average droplet size.

Span factors for 785 and 1200 rpm are not affected from the feed rate but for 850 rpm, the span factor decreases in 900 s due to bigger droplets turning into smaller droplets. While it was noted that the effect of feed rate is more pronounced at lower speeds, 850 rpm seems to be a more critical speed than 785 rpm for RT-T/2. This is because the span of distribution decreases and decrease in droplet size is slightly more in the case of feeding in 900 seconds. At 850 rpm possibly the increased particle-droplet collision frequency and particle attachment efficiency provide a better balance thereby, it leads to smaller droplets and a more uniform droplet size distribution.

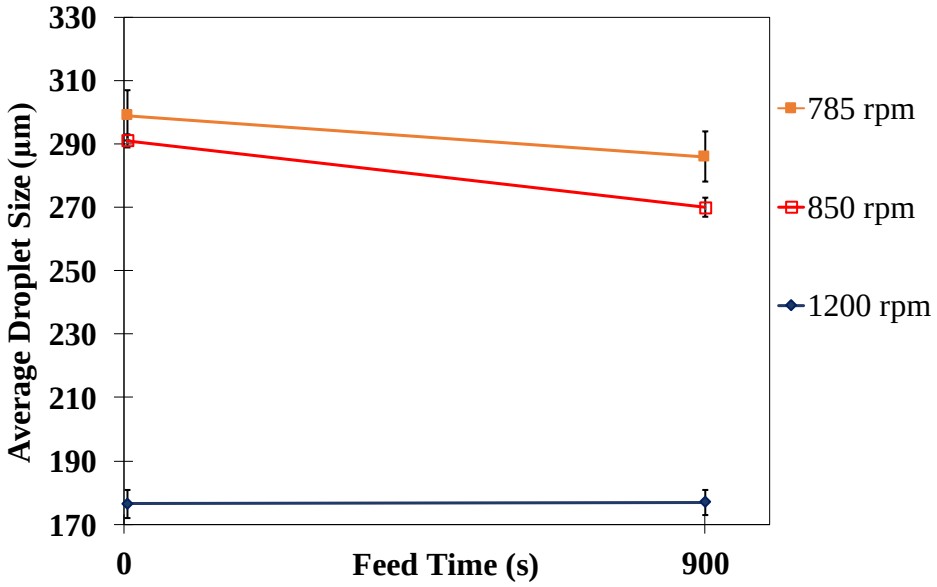

a.

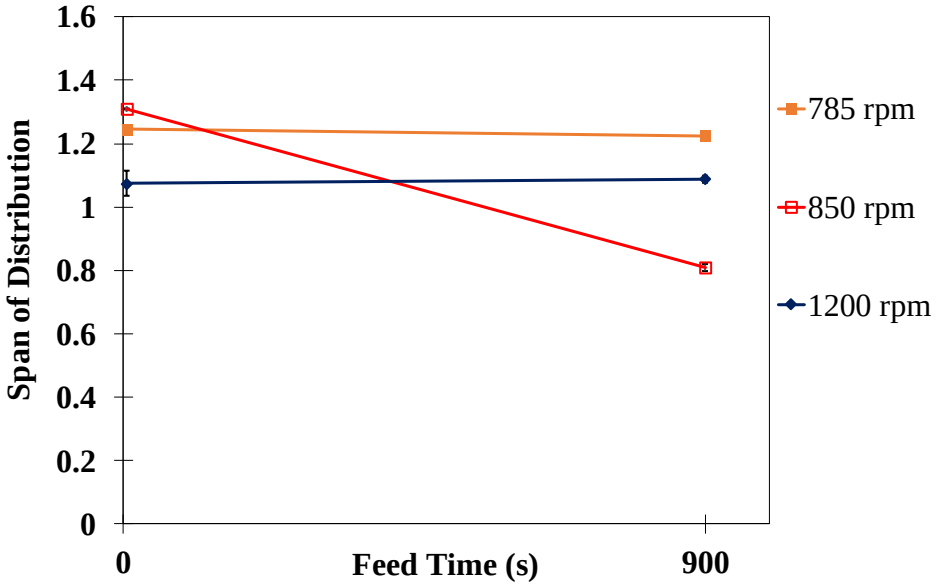

b.

Figure 3-6: Effect of feed rate on a. the average droplet size b. span of distribution at different impeller speeds for RT-T/2.

For PBTU-T/2, the effect of feed rate on the average droplet size is presented in Figure 3-7a. A slight decrease of 4% is observed at the lowest speed of 785 rpm in 900 seconds of feed which is in line with the findings of Figure 3-6a. The span of distribution is not affected from the feed rate.

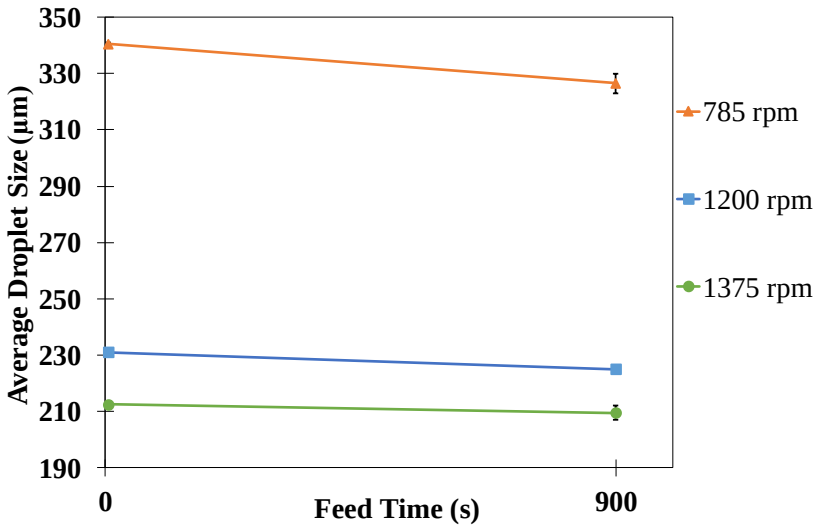

a.

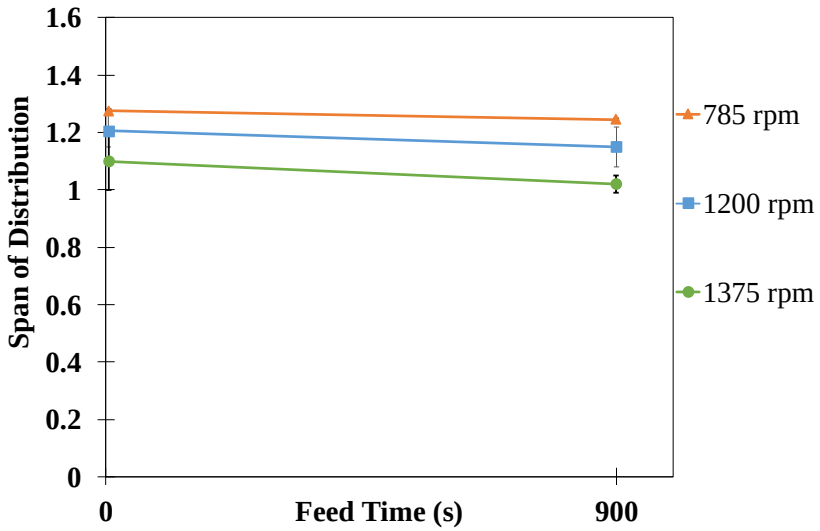

b.

Figure 3-7: Effect of feed rate at different impeller speeds on a. the average droplet size b. span of distribution for PBTU-T/2.

For PBTD-T/2, the effect of feed rate on the average droplet size and span of distribution are presented in Figure 3-8a and b. The average droplet size and span factor are not affected from the feed rate for all impeller speeds. The equilibrium is reached rapidly at all feed rates and impeller speeds of PBTD-T/2.

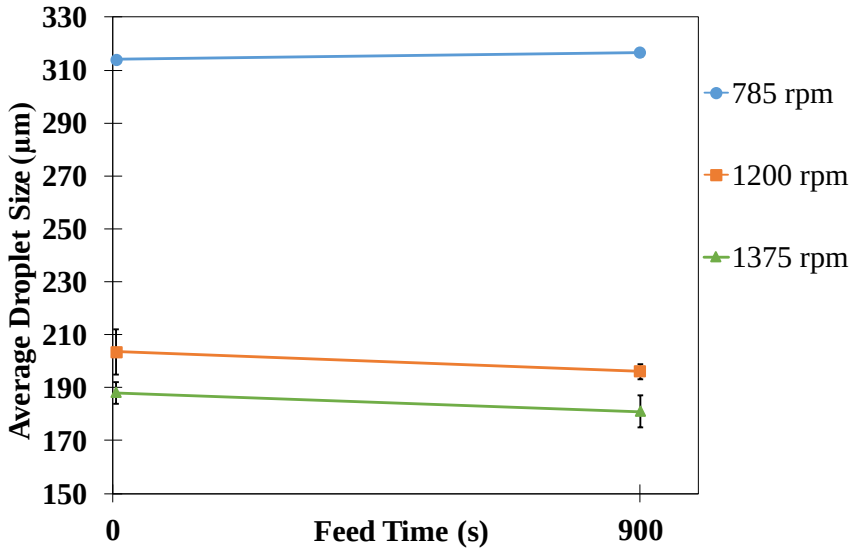

a.

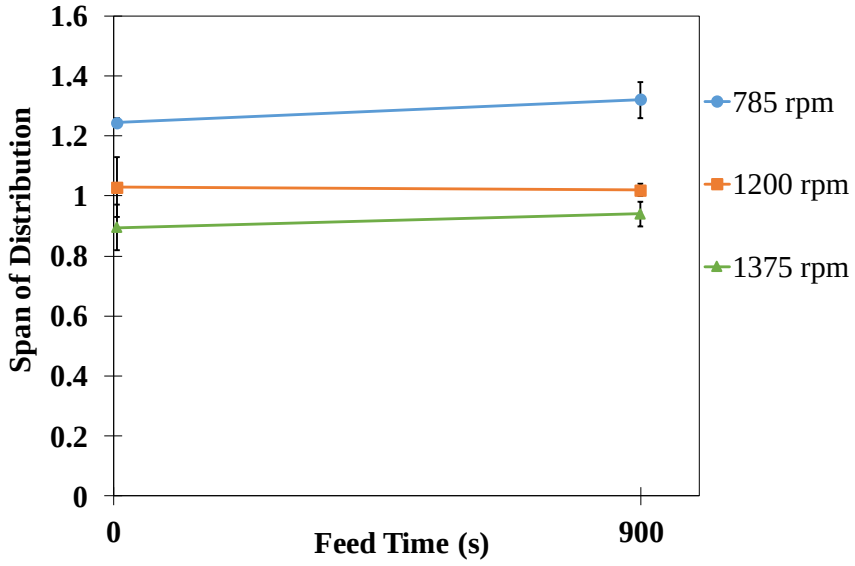

b.

Figure 3-8: Effect of feed rate at different impeller speeds on a. the average droplet size b. span of distribution for PBTD-T/2.

3.5 Effect of Lower Feed Rate on the Average Droplet Size

The findings in the previous sections showed that at low impeller speeds when oil is fed over 900 seconds rather than 5 seconds the average droplet sizes decrease slightly. To be able to observe the effect of feed time more clearly it is necessary to feed the oil over longer periods. RT-T/3 from Figure 3-4a is selected because the average droplet size is affected significantly from the change of feed rate; thereby, average droplet size can easily be observed with further decrease in feed rate (or increase in feed time).

Figure 3-9a shows the effect of feed time up to 3600 seconds on the average droplet size for the RT-T/3 at three different impeller speeds. The total change in the average droplet size from 5 to 3600 seconds is 24% at 1115 rpm and 10% at 1800 rpm. The major change is observed for the lower speed as expected. Lower impeller speeds increase the equilibrium time; therefore, the droplets reach equilibrium slowly at all feed times. As feed time is increased up to 3600 s, the newly generated droplets are much smaller than the other smaller feed times, and these droplets are covered by the particles effectively. This means that smaller average droplet sizes can be obtained at longer feed times.

The span of distribution is not affected for the higher impeller speed. However, for the lower impeller speed, the span factor increases with decreasing feed rate. This is due to the presence of the very small droplets that form at longer feed times, which leads to a d_{10} that is much smaller in value and much larger in volume. This, by definition, increases the span or also called as span factor.

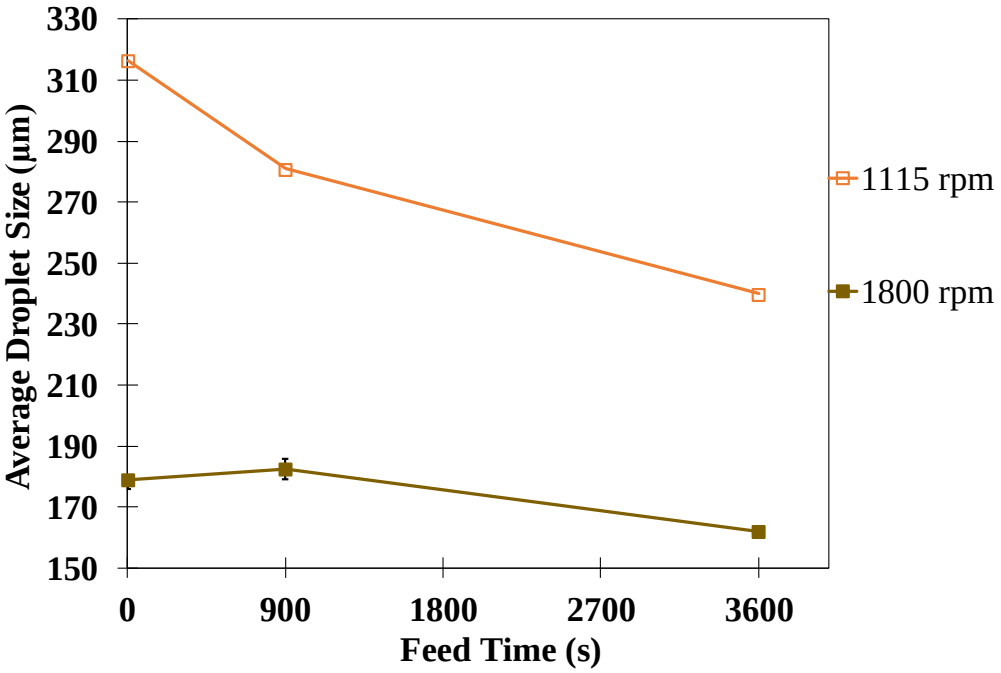

a.

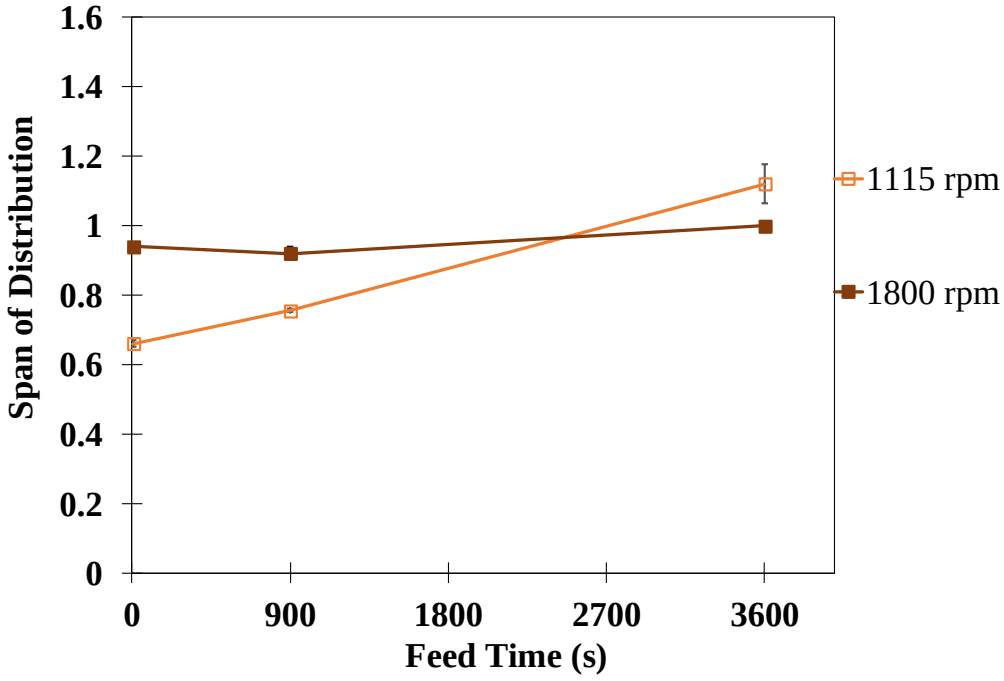

b.

Figure 3-9: Effect of lower feed rate on a. the average droplet size b. span of distribution for RT-T/3.

Up to this point, it was found that at the same tip speed both sizes of all impellers produce droplets that are close to each other in size which locates the droplet sizes to a somewhat expected range. Also, when the impeller speed is decreased the effect of feed time (feed rate) is more visible. Tip speed is directly proportional to the impeller speed. This indicates that if a fixed low tip speed is used and the oil is fed at long times, it would be possible to observe a change in the average droplet size at longer feed times even for impellers with which no effect was observed at higher tip speeds and shorter feed times. An example of this is the data for the T/2 impellers in Figure 3-3a where no effect of feed rate on droplet size was observed. To test the aforementioned hypothesis, the experiments for the T/2 impellers in Figure 3-3a were run at a lower tip speed (V_{tip}=2.03 m/s) and longer feed time (3600 s) for the three impellers. The results are given in Figure 3-10a. As feed time is increased to 3600 s the average droplet sizes with all impellers decreased visibly under these conditions. The total changes in the average droplet sizes from 5 to 3600 s are: 8% for PBTU-T/2, 8% for PBTD-T/2 and 11% for RT-T/2. The smallest average droplet size and major difference is observed with RT-T/2. This is a result of the higher shear level of RT-T/2.

For impeller type comparison, the decreasing order of average droplet size is the same as Figure 3-3a: PBTU, PBTD and RT. This shows that the decrease in the tip speed does not change the order of average droplet size.

The span of distribution is not affected from the feed rate for all type of impellers and their span factors are very similar to each other as illustrated in Figure 3-10b.

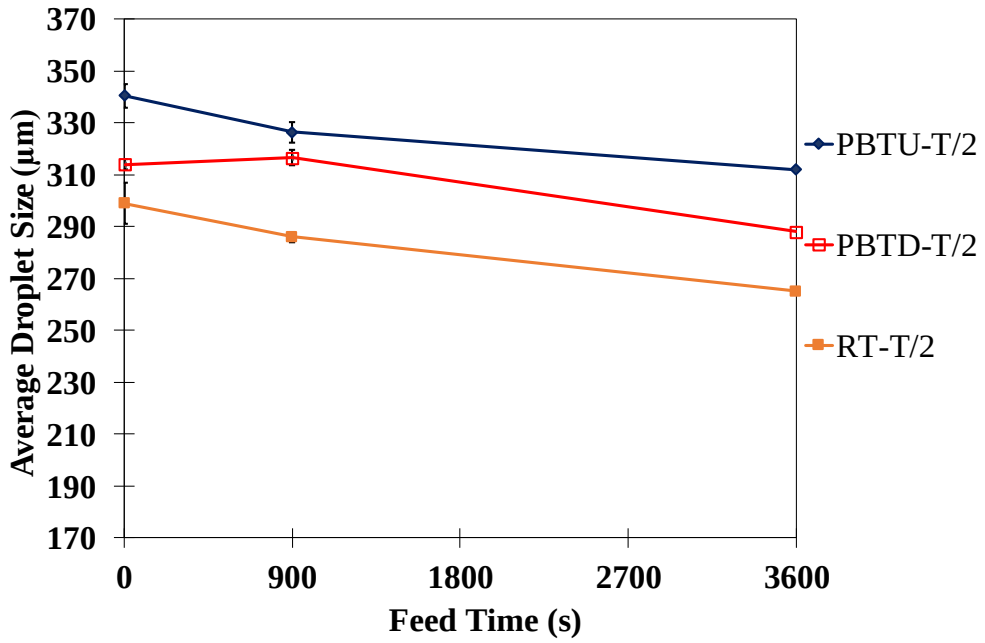

a.

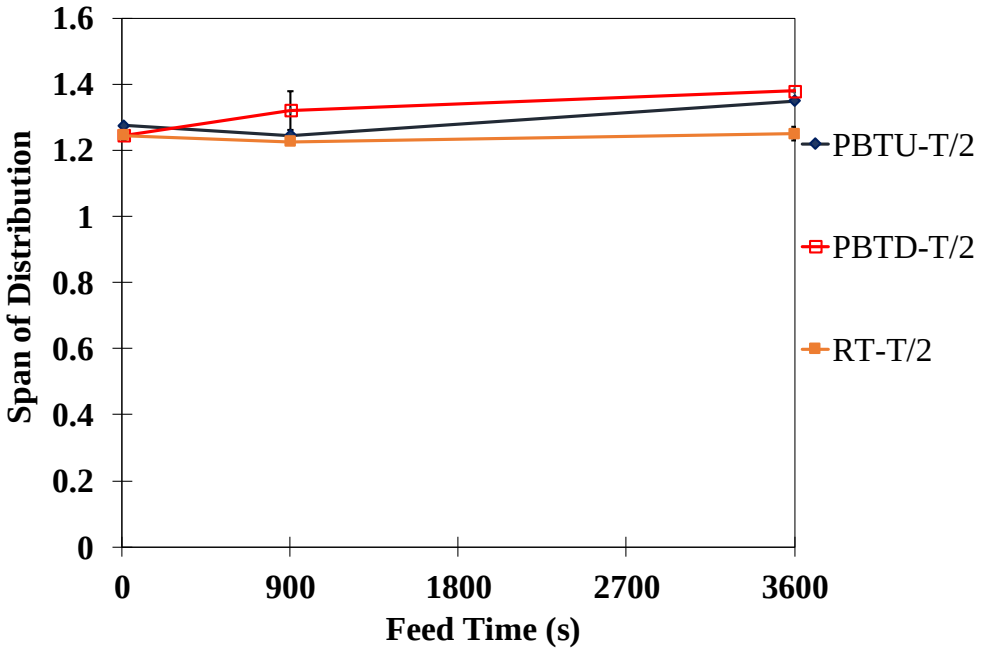

b.

Figure 3-10: Effect of lower feed rate on a. the average droplet size b. span of distribution at constant tip speed of 2.03 m/s for T/2 impellers.

3.6 Overview of Pickering and Surfactant-Based Emulsions Production in Stirred Tanks

In this part, general behavior of Pickering emulsions that were produced based on various processing and design parameters in this study is compared with the behavior of surfactant-based and other Pickering emulsions in the literature. Before touching upon the effect of the parameters, it is important to highlight the main difference between these emulsions. The major difference between surfactant-based and Pickering emulsions is the stabilization mechanism. In Pickering emulsions, first, droplet generation mechanism occurs, and then solid particles adsorb at the interface of oil and water to prevent coalescence by forming a steric barrier. However, for surfactant-based emulsions, surfactant adsorption mechanism is faster and surfactant plays an important role for both droplet breakage by lowering the interfacial tension and preventing the coalescence of freshly generated droplets (Tsabet & Fradette, 2015). In both types of emulsion, emulsification is a dynamic process and occurs in microsecond range (Tadros, 2013).

Effect of dispersed phase addition point on the average droplet size is studied with silicone oil in water and surfactant solution by EL-Hamouz et al. (2009). It is stated that effect of addition points is less pronounced at higher impeller speeds for surfactant-based emulsions. At higher impeller speeds, first stage of oil draw down to the impeller is not dominant as at the lower speeds. Thereby, addition of the oil from surface or impeller zone does not matter at higher speeds. This behavior is also valid for Pickering emulsion production as discussed in Section 3.2.

Emulsification processes are very sensitive to incorporation speed of dispersed phase into continuous phase. For surfactant-based emulsions, Jahanzad et al. (2010) studied the effect of addition time (feed rate) of the dispersed phase on type of inversion and the average droplet size. However, in the present study, phase inversion is undesirable. Therefore, these studies are compared only in terms of effect of addition rate of second phase into first phase on droplet size. In both types of emulsions, slow addition time produces smaller droplets if the droplets have not already reached minimum equilibrium size. Manga et al. (2017) also studied the effect of dispersed

phase feed rate on droplet diameter. In this study, different from the previous study, stirred cell membrane emulsification with solid particles was utilized. It is found that when oil flux (oil feed rate through the membrane cross-section) is decreased, smaller droplets are obtained because oil flux controls generation of new interfacial area as in the case of the present study.

The effect of impeller type on the average droplet size is considered at constant power per mass and tip speed for both types of emulsions. Pacek et al. (1999) showed that the low power number impellers with equal sizes produce smaller droplet sizes at the same power per mass in the case of liquid-liquid system without surfactants. EL-Hamouz et al. (2009) and Podgórska (2009) showed that in the case of liquid-liquid system with a surfactant, smaller droplets are produced with PBT than with RT when the power per mass is the same. In the present case, these findings agree also with Pickering emulsion production in stirred tanks. This means that PBTD is the most effective impeller in terms of power consumption for both types of emulsion.

For constant tip speed, EL-Hamouz et al. (2009), who studied with silicone oil-water dispersions in presence of surfactant, stated that low power impeller which is Sawtooth impeller produces smaller droplet sizes compared to PBT which is considered as high power impeller for that study. These were defined according to power number of the impellers. The outcome of EL-Hamouz et al. (2009) study is contrary to findings of the Pickering emulsions in this thesis and previous studies since at constant tip speed high power impeller which is PBT should have produced smaller droplets due to higher energy input. The reason of the difference is stated as having more shearing points of the Sawtooth impeller at high shear rates compared to PBT. Thus, it cannot certainly be said that high power impeller yields the smaller droplet sizes without considering the special types of the low power impeller. EL-Hamouz et al. (2009) also studied relation of average droplet size with tip speed and power per mass. It is stated that tip speed has better means of prediction in surfactant-based emulsions. In this thesis, tip speed was also found as a better choice for relating the average droplet size compared to other hydrodynamic parameters as a starting point of deriving correlations.

CHAPTER 4

SUMMARY, OUTCOMES AND FUTURE WORK

4.1 Summary and Outcomes

The influence of feed rate on production of Pickering emulsions at constant hydrodynamic parameters of tip speed, power per mass and Reynolds number were investigated. In the experiments, three most-conventional impeller types which are RT, PBTD and PBTU of T/2 and T/3 sizes were utilized. Concentrated emulsions (33 wt. %) were prepared in the baffled tank with specially designed lid in order to study the effect of dispersed phase feed rate on average droplet size as well as other parameters such as emulsification time, feeding point, impeller type and size and hydrodynamic parameters. The performance of the emulsions was characterized by comparing average droplet sizes which were measured in Mastersizer® 3000 (Malvern).

Important outcomes of the study can be summarized as follows:

- After 2 hours of emulsification, the average droplet sizes are not affected significantly from the emulsification time for all impellers at a tip speed of 3.11 m/s since an equilibrium between droplet breakage, particle adsorption and coalescence is reached.
- The effect of feed point was evaluated for the T/2 impellers. The smallest average droplet sizes are obtained at the point of higher local energy dissipation compared to the other points. However, feeding the oil from only the surface point gives similar average droplet size as in the case of feeding from higher local energy dissipation point. This shows that when the feed rate is changed, the effect of feed rate on average droplet size is more pronounced whether the oil is fed from the surface or impeller vicinity. This finding may

be related to the high mixing intensity under these conditions, which allows the system to reach equilibrium rapidly.

- It is concluded that tip speed gives better prediction than power per mass or Reynolds number since the gap in average droplet sizes among different impellers is smaller compared to other hydrodynamic parameters. However, power per mass becomes a crucial parameter when different types of impellers are compared in terms of power consumption
- T/2 impellers provide stronger circulation than T/3 impellers due to higher tip speed at constant power per mass of 243 W/kg. However, increasing the feed time from 5 s to 900 s removes the effect of impeller diameter. Both T/2 and T/3 impellers produce equal average droplet size in the case of 900 s feeding.
- The results indicate that the selection of the most effective impeller for Pickering emulsions is not straightforward. At constant tip speed, RT produces smaller average droplet size since it has higher energy input compared to PBT. However, it is better to select low power impeller which is PBTD if the concern is lower energy consumption. This is because PBTD produces smaller average droplet size at constant power per mass. PBTU is also low power impeller but the droplets generated with PBTU tend to stay in coalescence zone because of the flow pattern. This increases the circulation time and an increase in circulation time leads to larger average droplet size.
- The feed rate of dispersed phase controls the size of newly generated droplets. Thereby, the average droplet size can further be decreased with RT, PBTD and PBTU by lowering the feed rates if the droplets have not already reached the equilibrium size at different hydrodynamic parameters. Also, the reduction in average droplet size by decreasing feed rate is more pronounced at lower impeller speeds. This is because lower impeller speeds increase the equilibrium time; therefore, the average droplet size does not reach equilibrium rapidly at lower impeller speeds. At longer feed time (3600 s) and lower impeller speeds (1115 rpm), the maximum reduction in average droplet size is 24% with RT-T/3.

4.2 Future Work

The study presented in this thesis mainly focused on the effect of processing parameters especially the dispersed phase feed rate, design and hydrodynamic parameters in a stirred tank on the production of Pickering emulsions. However, there are several arising research topics based on this work. The following are listed to be pursued in a future study:

- Weber number is also a significant hydrodynamic parameter for predicting the average droplet size in liquid-liquid dispersions; therefore, the effect of dispersed phase feed rate on the average droplet size can be investigated at constant Weber number. In addition, the results can be compared with this work for deriving correlations to predict the average droplet size.
- Different types of particles and oil can be used to test the behavior of Pickering emulsion production at different feed rates, thereby the results can be compared with this work. It can be decided whether the behavior depends on particle and oil type. Also, contact angle measurements can be done by using contact angle gonimeter.
- With a type of eligible pump such as syringe pump that has capacity to supply the oil at longer feed times (longer than 3600 s), the effect of dispersed phase feed rate can be investigated in lower feed rates.

REFERENCES

Afshar Ghotli, R., Raman, A. A. A., Ibrahim, S., & Baroutian, S. (2013). Liquid-Liquid Mixing in Stirred Vessels: a Review. *Chemical Engineering Communications*, *200*(5), 595–627.

Ali, A. M., Yuan, H. H. S., Dickey, D. S. and Tattemn, G. B. (1981). Liquid dispersion mechanisns in agitated tanks: Part 1. pitched blade turbine. *Chem. Eng. Commu*, (10), 205–213.

Arditty, S., Whitby, C. P., Binks, B. P., Schmitt, V., & Leal-Calderon, F. (2003). Some general features of limited coalescence in solid-stabilized emulsions. *European Physical Journal E.*, *12*(2), 355–355.

Assirelli, M., Bujalski, W., Eaglesham, A., & Nienow, A. W. (2002). Study of micromixing in a stirred tank using a Rushton turbine: Comparison of feed positions and other mixing devices. *Chemical Engineering Research and Design*, *80*(8), 855–863.

Bhattacharya, S., & Kresta, S. M. (2004). Surface feed with minimum by-product formation for competitive reactions. *Chemical Engineering Research and Design*, *82*(9 SPEC. ISS.), 1153–1160.

Binks, B. P., & Lumsdon, S. O. (2000). Catastrophic phase inversion of water-in-oil emulsions stabilized by hydrophobic silica. *Langmuir*, *16*(6), 2539–2547.

Binks, B. P., & Lumsdon, S. O. (2001). Pickering emulsions stabilized by monodisperse latex particles: Effects of particle size. *Langmuir*, *17*(15), 4540–4547.

Binks, B. P. (2002). Particles as surfactants - Similarities and differences. *Current Opinion in Colloid and Interface Science*, *7*(1–2), 21–41.

Calabrese, R V. (1979). The effect of dispersed phase viscosity on drop breakup in agitated liquid-liquid systems. In *Joint Japanese-North American Mixing Conference, AIChE, 72nd Annual Meeting*.

Calabrese, R. V., Chang, T. P. K., & Dang, P. T. (1986). Drop breakup in turbulent stirred tank contactors. Part I: Effect of dispersed phase viscosity. *AIChE Journal*, *32*(4), 657–666.

Chappat, M. (1994). Some applications of emulsions. *Colloids and Surfaces A: Physicochemical and Engineering Aspects*, *91*(C), 57–77.

Chapple, D., Kresta, S. M., Wall, A., & Afacan, A. (2002). The effect of impeller and tank geometry on power number for a pitched blade turbine. *Chemical Engineering Research and Design*, *80*(4), 364–372.

Chen, H. T., & Middleman, S. (1967). Drop Size Distribution in Agitated Liquid-Liq uid Systems. *AIChE Journal*, *13*(5), 989–995.

D. Langevin, S. Poteau, I. H. and J. F. A. (2004). Crude Oil Emulsion Properties and their Application to Heavy Oil Transportation. *Oil & Gas Science and Technology-Revue*, *59*, 511–521.

Davies, J. T. (1985). Drop sizes of emulsions related to turbulent energy dissipation rates. *Chemical Engineering Science*, *40*(5), 839–842.

Doran, P. M. (2013). Functions of Mixing. In *Bioprocess Engineering Principles (Second Edition)* (pp. 255–332). *Elsevier.*

EL-Hamouz, A., Cooke, M., Kowalski, A., & Sharratt, P. (2009). Dispersion of silicone oil in water surfactant solution: Effect of impeller speed, oil viscosity and addition point on drop size distribution. *Chemical Engineering and Processing: Process Intensification*, *48*(2), 633–642.

Frelichowska, J., Bolzinger, M. A., Valour, J. P., Mouaziz, H., Pelletier, J., and Chevalier, Y. y. (2009). Pickering w/o emulsions: drug release and topical delivery. *Int. J. Pharm.*, *368*, 7–15.

Ghotli, R. A., Raman, A. A. A., & Ibrahim, S. (2013). LIQUID-LIQUID MIXING IN STIRRED VESSELS: A REVIEW. *Chemical Engineering Communications*, *200*, 595–627.

Golemanov, K., Tcholakova, S., Kralchevsky, P. A., Ananthapadmanabhan, K. P., & Lips, A. (2006). Latex-particle-stabilized emulsions of anti-Bancroft type. *Langmuir*, *22*(11), 4968–4977.

Hemrajani, R. R., & Gary B., T. (2004). Mechanically Stirred Vessels.In: Paul EL, Atiemo-Obeng VA, Kresta. SM, eds. In *Handbook of Industrial Mixing: Science and Practice*.

Hinze, J., & Shell-laboratory, R. D. (1955). Fundamentals of the Hydrodynamic Mechanism of Splitting in Dispersion Processes. *AIChE Journal*, *1*(3), 289–295.

Jahanzad, F., Josephides, D., Mansourian, A., & Sajjadi, S. (2010). Dynamics of transitional phase inversion emulsification: Effect of addition time on the type of inversion and drop size. *Industrial and Engineering Chemistry Research*, *49*(16), 7631–7637.

Jakobsen, H. A. (2008). Agitation and Fluid Mixing Technology.In *Chemical reactor modeling*. *Springer*.

James Y. Oldshue. (1986). Fluid mixing technology. *AIChE Journal*, *32*, 1403–1403.

Joseph, Daniel D.; Wang, J.; Bai, R.; Yang, B. H.; and Hu, H. H. (2003). Particle Motion in a Liquid Film Rimming the Inside of a Partially Filled Rotating Cylinder. *Journal of Fluid Mechanics*, *496*, 139–163.

Larsson, K., & Friberg, S. E. (1990). *Food emulsions*. Retrieved from http://www.cabdirect.org/abstracts/19910445562.html;jsessionid=F1B238C4FB6F0D642B12BC92C9788F1A?freeview=true

Lemenand, T., Della Valle, D., Zellouf, Y., and Peerhossaini, H. (2003). Droplet formation in turbulent mixing of two immiscible fluids in a new type of static mixer. *Int. J. Multiph. Flow*, *29*, 813–840.

Leng, D. E., & Calabrese, R. V. (2004). Immiscible Liquid–Liquid Systems. In: Paul EL, Atiemo-Obeng VA, Kresta. SM, eds. In *Handbook of Industrial Mixing: Science and Practice*. *John Wiley & Sons.*

Levine, S., & Bowen, B. D. (1991). Capillary Interaction of Spherical-Particles Adsorbed on the Surface of an Oil-Water Droplet Stabilized by the Particles 1. *Colloids and Surfaces*, *59*, 377–386.

Levine, S., Bowen, B. D., & Partridge, S. J. (1989). Stabilization of Emulsions by Fine Particles 1. Partitioning of Particles between Continuous Phase and Oil-Water Interface. *Colloids & Surfaces*, *38*(4), 325–343.

Madivala, B., Vandebril, S., Fransaer, J., & Vermant, J. (2009). Exploiting particle shape in solid stabilized emulsions. *Soft Matter*, *5*(8), 1717–1727.

Mahdi Jafari, S., He, Y., & Bhandari, B. (2006). Nano-emulsion production by sonication and microfluidization - A comparison. *International Journal of Food Properties*, *9*(3), 475–485.

Marden, E., & Bakker, M. and A. (2004). Computational Fluid Mixing.In: Paul EL, Atiemo-Obeng VA, Kresta. SM, eds. In *Handbook of Industrial Mixing: Science and Practice.*

Marto, J., Gouveia, L., Jorge, I. M., Duarte, A., Goncalves, L. M., Silva, S. M., et al. (2015). Starch-based Pickering emulsions for topical drug delivery: a QbD approach. Colloids Surf. B Biointerfaces, *135*, 183–192.

McManamey, W. J. (1979). Sauter mean and maximum drop diameters of liquid-liquid dispersions in turbulent agitated vessels at low dispersed phase hold-up. *Chemical Engineering Science*, *34*(3), 432–434.

Mohamed. S. Manga and David. W. York. (2017). Production of Concentrated Pickering Emulsions with Narrow Size Distributions Using Stirred Cell Membrane Emulsification. *Langmuir*, *33*, 9050−9056.

O'Rourke, A. M., & MacLoughlin, P. F. (2005). A comparison of measurement techniques used in the analysis of evolving liquid-liquid dispersions. *Chemical Engineering and Processing: Process Intensification*, *44*(8), 885–894.

Pacek A.W., Chamsart S., Nienow A.W., B. A. (1999). The Influence of Impeller Type on Mean Drop Size and Drop Size Distribution in an Agitated Vessel. *Chem. Eng. Sci.*, *54*, 4211–4222.

Paul, E. L., & Victor A. Atiemo-Obeng, and S. M. K. (2004). *Introduction. In: Paul EL, Atiemo-Obeng VA, Kresta. SM, eds. Handbook of Industrial Mixing: Science and Practice*. *John Wiley & Sons, Inc.*

Pawlik, A., Kurukji, D., Norton, I., & Spyropoulos, F. (2016). Food-grade Pickering emulsions stabilised with solid lipid particles. *Food and Function*, *7*(6), 2712–2721.

Pickering, S. U. (1907). Emulsions. *J. Chem. Soc., Trans.*, *91*, 2001–2021.

Podgórska, W. (2009). Prediction of Drop Size Distributions in Stirred Tanks Equipped With Radial-and Axial Flow Impellers. *Chemical and Process Engineering*,181–197.

Princen, H. ., Zia, I. Y. ., & Mason, S. . (1967). Measurement of interfacial tension from the shape of a rotating drop. *Journal of Colloid and Interface Science*, *23*(1), 99–107.

Ramsden, W. (1903). Separation of solids in the surface-layers of solutions and suspensions. *Proceedings of the Royal Society of London*, *72*, 156–164.

Roscoe, R. (1952). The viscosity of suspensions of rigid spheres. *Br J Appl Phys*, *3*, 267.

Tadros, T. F. (2013). Emulsion Formation,Stability, and Rheology. *Emulsion Formation and Stability*, 1–76. *John Wiley & Sons*

Tarimala, S., & Dai, L. L. (2004). Structure of microparticles in solid-stabilized emulsions. *Langmuir*, *20*(9), 3492–3494.

Timothy Hirzel. (n.d.). PWM. Retrieved June 4, 2018, from https://www.arduino.cc/en/Tutorial/PWM

Tsabet, E. (2014). *De La Particule Au Procédé: Modélisation De La Production D'émulsions De Pickering*. Université De Montréal, Dissertation Thesis.

Tsabet, E., & Fradette, L. (2015). Effect of Processing Parameters on the Production of Pickering Emulsions. *Ind. Eng. Chem. Res*, *54*, 2227−2236.

Weetman, R. J. (2004). Role of the Mixing Equipment Supplier.In: Paul EL, Atiemo-Obeng VA, Kresta. SM, eds. In *Handbook of Industrial Mixing: Science and Practice*. *John Wiley & Sons, Inc.*

Xu, R. (2000). Electrophoretic Light Scattering - Zeta Potencial Measurement. *Particle Characterization: Light Scattering Methods*, 289–343.

Yan, N. X., & Masliyah, J. H. (1996). (1996). Effect of pH on adsorption and desorption of clay particles at oil-water interface. *Journal of Colloid & Interface Science*, *181*(1), 20–27.

Yan, N. X., Gray, M. R., & Masliyah, J. H. (2001). On water-in-oil emulsions stabilized by fine solids. *Colloids and Surfaces A: Physicochemical and Engineering Aspects*, *193*(1–3), 97–107.

Yang, Y., Fang, Z., Chen, X., Zhang, W., Xie, Y., Chen, Y., … Yuan, W. (2017). An overview of pickering emulsions: Solid-particle materials, classification, morphology, and applications. *Frontiers in Pharmacology*, *8*(5), 1–20.

Yoshida, M., Ebina, H., Shirosaki, H., Ishioka, K., & Oiso, K. (2015). Liquid flow in impeller swept regions of baffled and unbaffled vessels with a turbine-type agitator. *Brazilian Journal of Chemical Engineering*, *32*(4), 865–873.

Zhao, Y., Li, X., Cheng, J., Yang, C., & Mao, Z. S. (2011). Experimental study on liquid-liquid macromixing in a stirred tank. *Industrial and Engineering Chemistry Research*, *50*(10), 5952–5958.

Zhou, G. (1997). Characteristics of Turbulence Energy Dissipation and Liquid-Liquid Dispersions in An Agitated Tank.University of Alberta. Dissertation Thesis.

Zhou, G., & Kresta, S. M. (1998). Correlation of mean drop size and minimum drop size with the turbulence energy dissipation and the flow in an agitated tank. *Chemical Engineering Science*, *53*(11), 2063-2079.

APPENDIX

A. Impeller Dimensions

Impeller dimensions are adapted to the system from Chapple et al. (2002) for RT and for PBT. Impeller drawings and dimensions are shown in Figure A-1 and A-2, Table A-1 and Table A-2, respectively. Figures were not drawn to scale since T/3 and T/2 impellers were used.

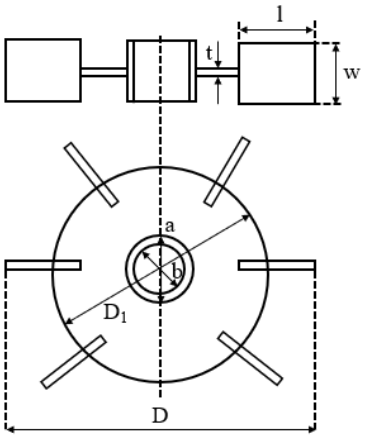

Figure A-1: Detail drawing for RT

Table A-1: Dimensions of RT

Tank Diameter (T)	T=9.9 mm
Impeller Diameter (D)	T/2, T/3
Hub Diameter (a)	D/6.3
Hub Bore (b)	D/12.6
Hub Height	D/5.6
Blade Thickness (t)	D/90.9
Blade Width (w)	D/5
Blade Length	D/4
Disk Diameter	D/1.5
Disk Thickness	D/58.8

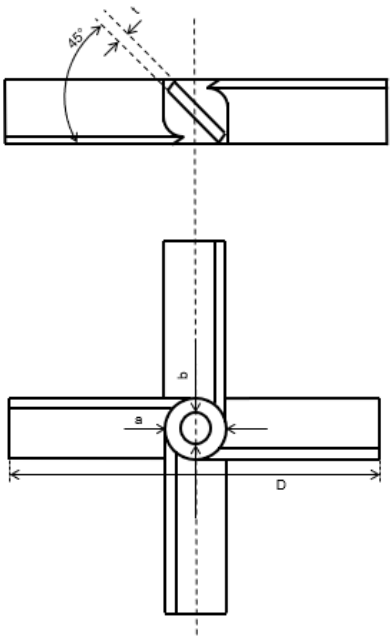

Figure A-2: Detail drawing for PBT

Table A-2: Dimensions of PBT

Tank Diameter (T)	T=9.9 mm
Impeller Diameter (D)	T/2, T/3
Hub Diameter (a)	D/4
Hub Bore (b)	D/8.7
Hub Height	D/5.6
Blade Thickness (t)	D/26.7
Blade Width (w)	D/5

B. Feed Rate Controller Source Code

```
function varargout = GUI(varargin)
% GUI MATLAB code for GUI.fig
% GUI, by itself, creates a new GUI or raises the existing
% singleton*.
%
% H = GUI returns the handle to a new GUI or the handle to
% the existing singleton*.
%
% GUI('CALLBACK',hObject,eventData,handles,...) calls the local
% function named CALLBACK in GUI.M with the given input arguments.
%
% GUI('Property','Value',...) creates a new GUI or raises the
% existing singleton*. Starting from the left, property value pairs are
% applied to the GUI before GUI_OpeningFcn gets called. An
% unrecognized property name or invalid value makes property application
% stop. All inputs are passed to GUI_OpeningFcn via varargin.
%
% *See GUI Options on GUIDE's Tools menu.  Choose "GUI allows only one
% instance to run (singleton)".
%
% See also: GUIDE, GUIDATA, GUIHANDLES

% Edit the above text to modify the response to help GUI

% Last Modified by GUIDE v2.5 05-Oct-2017 22:47:51

% Begin initialization code - DO NOT EDIT
gui_Singleton = 1;
gui_State = struct('gui_Name', mfilename, ...
'gui_Singleton', gui_Singleton, ...
```

```
'gui_OpeningFcn', @GUI_OpeningFcn, ...
'gui_OutputFcn', @GUI_OutputFcn, ...
'gui_LayoutFcn', [] , ...
'gui_Callback', []);
if nargin && ischar(varargin{1})
gui_State.gui_Callback = str2func(varargin{1});
end

if nargout
[varargout{1:nargout}] = gui_mainfcn(gui_State, varargin{:});
else
gui_mainfcn(gui_State, varargin{:});
end
% End initialization code - DO NOT EDIT

% --- Executes just before GUI is made visible.
function GUI_OpeningFcn(hObject, eventdata, handles, varargin)
% This function has no output args, see OutputFcn.
% hObject handle to figure
% eventdata reserved - to be defined in a future version of MATLAB
% handles structure with handles and user data (see GUIDATA)
% varargin command line arguments to GUI (see VARARGIN)
instrreset;
handles.balance=serial('COM4','BaudRate',9600);
handles.ardu=serial('COM3','BaudRate',9600);
fopen(handles.ardu);
%fopen(handles.balance);
% Choose default command line output for GUI
handles.output = hObject;
```

```
% Update handles structure
guidata(hObject, handles);

% UIWAIT makes GUI wait for user response (see UIRESUME)
% uiwait(handles.figure1);

% --- Outputs from this function are returned to the command line.
function varargout = GUI_OutputFcn(hObject, eventdata, handles)
% varargout cell array for returning output args (see VARARGOUT);
% hObject handle to figure
% eventdata reserved - to be defined in a future version of MATLAB
% handles structure with handles and user data (see GUIDATA)

% Get default command line output from handles structure
varargout{1} = handles.output;

function curWeight=curWeightCalc(s1)

fopen(s1);
fprintf(s1,'IP');
pause(0.01)
% Take Data from balance
fscanf(s1);
fscanf(s1);
fscanf(s1);
fscanf(s1);
fscanf(s1);
fscanf(s1);
gr=fscanf(s1);
curWeight=str2num(gr(1:6));%in gr
```

```
fclose(s1);
% --- Executes on button press in pushbutton1.
function pushbutton1_Callback(hObject, eventdata, handles)
% hObject handle to pushbutton1 (see GCBO)
% eventdata reserved - to be defined in a future version of MATLAB
% handles structure with handles and user data (see GUIDATA)
timeSamp=1;
pwmEst=90;

estpwmPerkgs=pwmEst/14.4*2; %kg/s per pwm
errorInt=0;

flowRat=str2num(get(handles.flowRate,'String')); %in gr/s
dur=str2num(get(handles.expDur,'String'));

initialWeight=curWeightCalc(handles.balance);
set(handles.balanceCur,'String',num2str(initialWeight));

targetWeight=flowRat*dur*60;
set(handles.targetOil,'String',num2str(targetWeight));
set(handles.curFlow,'String',num2str(0.00));
set(handles.pumpedOil,'String',num2str(0.00));
set(handles.timeElap,'String',num2str(0.00));

%curWeightPre=initialWeight+flowRat*timeSamp;
flowRateCur=flowRat;
count=0;
pumpedOil=0;
fprintf(handles.ardu,'%u',pwmEst);
tIni=tic;
set(handles.statu,'String','Running')
```

```
while targetWeight-pumpedOil>0.6
curWeight=curWeightCalc(handles.balance);
tcur=toc(tIni);
Wref=initialWeight-flowRat*tcur;
errorFlow=(curWeight-Wref)*estpwmPerkgs;
errorInt=errorInt+errorFlow;
a=double(int16(pwmEst+errorFlow+errorInt*0.1));
if a<85
a=85;
end
fprintf(handles.ardu,'%u',a);
set(handles.balanceCur,'String',num2str(curWeight))
set(handles.pwmShow,'String',num2str(a));
count=count+1;
pause(timeSamp-1+0.4);
set(handles.curFlow,'String',num2str(curWeight-Wref));
set(handles.pumpedOil,'String',num2str(pumpedOil));
set(handles.timeElap,'String',num2str(toc(tIni)));
pumpedOil=initialWeight-curWeight;
end

fprintf(handles.ardu,'%u',0);
set(handles.timeElap,'String',num2str(toc(tIni)));
pause(2);
set(handles.statu,'String','Completed')
curWeight=curWeightCalc(handles.balance);
set(handles.balanceCur,'String',num2str(curWeight));
pumpedOil=initialWeight-curWeight;
set(handles.pumpedOil,'String',num2str(pumpedOil));
```

```
function flowRate_Callback(hObject, eventdata, handles)
% hObject handle to flowRate (see GCBO)
% eventdata reserved - to be defined in a future version of MATLAB
% handles structure with handles and user data (see GUIDATA)

% Hints: get(hObject,'String') returns contents of flowRate as text
% str2double(get(hObject,'String')) returns contents of flowRate as a double

% --- Executes during object creation, after setting all properties.
function flowRate_CreateFcn(hObject, eventdata, handles)
% hObject handle to flowRate (see GCBO)
% eventdata reserved - to be defined in a future version of MATLAB
% handles empty - handles not created until after all CreateFcns called

% Hint: edit controls usually have a white background on Windows.
% See ISPC and COMPUTER.
if ispc && isequal(get(hObject,'BackgroundColor'),
get(0,'defaultUicontrolBackgroundColor'))
set(hObject,'BackgroundColor','white');
end

function expDur_Callback(hObject, eventdata, handles)
% hObject handle to expDur (see GCBO)
% eventdata reserved - to be defined in a future version of MATLAB
% handles structure with handles and user data (see GUIDATA)

% Hints: get(hObject,'String') returns contents of expDur as text
% str2double(get(hObject,'String')) returns contents of expDur as a double

% --- Executes during object creation, after setting all properties.
function expDur_CreateFcn(hObject, eventdata, handles)
```

```
% hObject handle to expDur (see GCBO)
% eventdata reserved - to be defined in a future version of MATLAB
% handles empty - handles not created until after all CreateFcns called

% Hint: edit controls usually have a white background on Windows.
% See ISPC and COMPUTER.
if ispc && isequal(get(hObject,'BackgroundColor'),
get(0,'defaultUicontrolBackgroundColor'))
set(hObject,'BackgroundColor','white');
end
```

ARDNUIO Source Code

```
*/

// Clockwise and counter-clockwise definitions.
// Depending on how you wired your motors, you may need to swap.
int num = 0;

#define FORWARD  0
#define REVERSE 1

// Motor definitions to make life easier:
#define MOTOR_A 0
#define MOTOR_B 1

// Pin Assignments //
//Default pins:
#define DIRA 2 // Direction control for motor A
#define PWMA 3  // PWM control (speed) for motor A
#define DIRB 4 // Direction control for motor B
```

```
#define PWMB 11 // PWM control (speed) for motor B

void setup()
{
  setupArdumoto(); // Set all pins as outputs
    digitalWrite(DIRA, 1);

}

char setPWM[3];
char dur[3];
unsigned int i = 0;

void loop()
{
    analogWrite(PWMA, num);
    delay(40);
    analogWrite(PWMA, 0);
    delay(40);

   //driveArdumoto(MOTOR_A, FORWARD, num);
       //delay(1);
     //   driveArdumoto(MOTOR_A, FORWARD, 0);
         //       delay(1);

  if (Serial.available() > 0) {
    Serial.setTimeout(10);

  //for (count=1;count<len;count++
  setPWM[0] = 0; setPWM[1] = 0; setPWM[2] = 0;
  dur[0] = 0; dur[1] = 0; dur[2] = 0;
```

```
    int len = Serial.readBytes(setPWM, 8);

    num = atoi(setPWM);
    if (num > 255) // saturate
      num = 255;
    if (num < 0)
      num = 0;

  }
}

//}

// setupArdumoto initialize all pins
void setupArdumoto()
{
  Serial.begin(9600);
  // All pins should be setup as outputs:
  pinMode(PWMA, OUTPUT);
  pinMode(PWMB, OUTPUT);
  pinMode(DIRA, OUTPUT);
  pinMode(DIRB, OUTPUT);
  // Initialize all pins as low:
  digitalWrite(PWMA, LOW);
  digitalWrite(PWMB, LOW);
  digitalWrite(DIRA, LOW);
  digitalWrite(DIRB, LOW);
}
```